Postprint of: Makurat-Kasprolewicz B., Ossowska A., Recent advances in electrochemically surface treated titanium and its alloys for biomedical applications: A review of anodic and plasma electrolytic oxidation methods, Materials Today Communications, Vol. 34 (2023), 105425, DOI: 10.1016/j.mtcomm.2023.105425.

Recent advances in electrochemically surface treated titanium and its alloys for biomedical applications: A review of anodic and plasma electrolytic oxidation methods

Balbina Makurat-Kasprolewicz [1,*], Agnieszka Ossowska [1]

[1] Gdansk University of Technology, Faculty of Mechanical Engineering and Ship Technology, 11/12 Narutowicza St., 80-233 Gdańsk
*** Correspondence: balbina.makurat-kasprolewicz@pg.edu.pl; tel.: +48-58-347-14-65**

Abstract

Nowadays, titanium and its alloys are widely used materials in implantology. Nevertheless, the greatest challenge is still its appropriate surface treatment in order to induce optimal properties, which facilitates formation of a permanent bond between the implant and human tissue. The use of electrochemical treatment such as anodic oxidation or plasma electrolytic oxidation allows for the production of porous coating that mimics the bone structure and accelerates the osseointegration process. The literature shows that the morphology, thickness, crystallinity, chemical composition, mechanical properties and corrosion resistance of coatings, as well as their bioactivity, strongly depend on the parameters of electrochemical processes (voltage, duration, composition and temperature of the electrolyte). The purpose of this study is to review, summarize, and analyze the latest accomplishments and trends in the development of coatings used in implantology, produced with the use of electrochemical oxidation and micro arc oxidation. Recent progress and future challenges associated with the surface modification of titanium and its alloy for biomedical applications have been discussed.

Keywords

anodic oxidation; micro-arc oxidation; plasma electrolytic oxidation; titanium alloys; biomedical application; implants

1. Introduction

Titanium and its alloys are widely used in medicine due to the diversity of their chemical composition and properties such as good biocompatibility, high chemical stability in the environment of tissue and body fluids, good fatigue resistance as well as high tensile and yield strengths (Fig. 1) [1]. Moreover, they exhibit extremely high corrosion resistance. This is by virtue of its affinity for oxygen, which has a positive effect on the formation of an impervious, tightly adjacent passive layer on its surface, composed mainly of oxides: TiO_2, Ti_2O_3 and TiO [2–4]. A particularly important parameter determining titanium and its alloys is the Young's modulus (Fig. 1). In the case of biomaterials, it should be as close as possible to the Young's modulus of the bone, because their mismatch may provoke stress shielding, which may result in loosening of the implant. As a consequence, it may lead to implant reoperation [4–8]. Despite the fact that titanium and its alloys show a lot of positive features in biomedical applications, there is still a problem with their bioactivity and mechanical properties even closer to those of bone (Fig. 1). In order to improve the properties of these metal biomaterials, it is crucial that a porous coating with an appropriate chemical and phase composition is formed on their surface [5–10]. A properly designed coating should have mechanical properties similar to the bone tissue of the person to be surgically treated. Establishing the ideal scaffold also involves imitating bone structure. In this case, the porosity of the resulting coating is very important as it determines the size and shape of the pores that have an impact on cell adhesion, proliferation and differentiation. Getting the perfect porous structure is a tremendous challenge for scientists [6,10–14].

Over the years, various surface treatment techniques have been proposed to produce a porous coating. Among them, there are physical (e.g. thermal spraying [15], plasma surface modification [16], ion implantation [17], physical vapour deposition [18]), chemical (e.g. sol-gel [19], chemical vapour deposition [20]) as well as electrochemical methods. Electrochemical methods have gained great popularity in recent times because they are relatively simple and cheap compared to other methods. In addition, they also allow for the deposition of a coating on implants of various shapes, and do not require specialized and expensive instrumentation. Furthermore, using electrochemical methods, it is possible to control the geometry of the coating and predict its mechanical properties. Anodic oxidation and micro-arc oxidation can be distinguished amid electrochemical methods [21–24]. Variable parameters such as voltage, processing time and current density, as well as the type of electrolyte allow scientists to adjust the properties of the coating to obtain a coating with the best properties [6,25–33]. In this article, the authors focus on the parameters of electrochemical processes and their influence on the properties of the resulting coating. They devote attention to the micro-arc oxidation technique, as it seems to be the most promising for biomedical application.

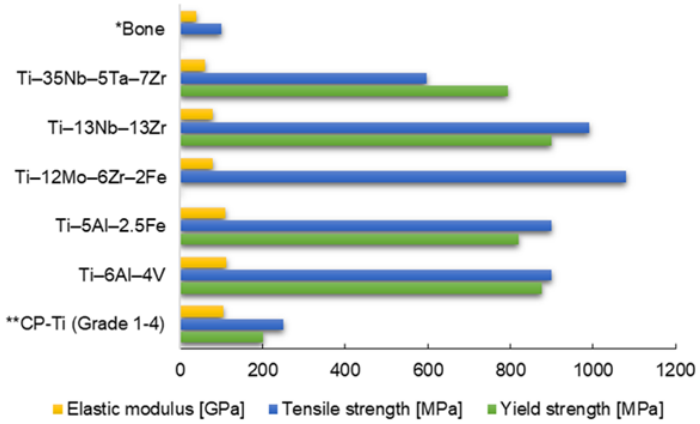

Fig. 1 Some biomechanical properties of titanium and its selected alloys in comparison with bone. *Variability depending on the type of bone and direction; **Approximate value for CP-Ti which depends on type of grade [1,3,5,6]. Designed and illustrated by the authors of the present work.

The issue of electrochemical treatment of titanium and its alloys is often discussed and characterized in the literature. Particular attention is paid to process parameters, electrolyte / suspension compositions, mechanical properties of coatings, chemical composition of coatings. Possible methods of surface modification of titanium and its titanium alloys as well as its properties are discussed [4,7,34–36]. The authors presented the influence of the anodizing process parameters on the mechanical properties of the obtained coatings [37–39], characterized the *in-vitro* and *in-vivo* assays of the resulting coatings [25,28,40]. In the case of micro-arc oxidation, the authors address special attention to the formation of coatings with incorporated various chemical elements with special properties, e.g. phosphorus [6,33], calcium [6,33], magnesium [6], silicon [41], silver [42], copper [43] or sodium [41], focusing on the study of the biomechanical properties and the ability to form apatite on coatings.

All the latest papers on optimization of electrochemical treatments can be applied to create porous coatings on titanium and its alloys. Despite the fact that these studies are at a very advanced level, it is still not possible to get answer to the critical question "which coating is consummately suited to the human body". Therefore, the purpose of this review is to present the latest accomplishments as well as an emerging trend in this field. This review allows to systematize the achievements and highlight the currently existing shortcomings. Most importantly, it focuses on characterizing relatively simple and cheap methods, the use of which results in coatings with promising properties useful in biomedicine. It shows not only the requirements for titanium implants, but also various process parameters for modification of its surface. The largest part is devoted to the comparatively recently introduced technique of micro-arc oxidation, which is derived from anodic oxidation. This overview also allows to find the differences between these two methods, i.e. conventional and modern views, as well as their advantages and disadvantages. The review focuses on titanium and its various alloys, showing the relationship between the parameters of a given technique and the mechanical, biological and chemical properties of the coating. Besides, challenges associated with the usage of titanium and its alloy in the field of biomaterials were discussed.

The methodology of preparing this article was based on several substitutes. Among them, the following can be distinguished: the subject of research (titanium and its alloys, anodic oxidation, micro-arc oxidation), publication data (mostly from the last 5 years), addressees (implantologists, surgeons, as well as biomedical, material and mechanical engineers) and published results (relationship between surface treatment parameters and electrolyte compositions, and mechanical, biological and chemical properties).

2. Anodic oxidation

The objective of anodic oxidation (or anodizing or electrochemical oxidation) is to modify the surface of the treated metal in an aqueous solution of electrolytes by creating an oxide layer under the influence of an external electric field. The formed coating can be solid or porous. Moreover, it is possible to form an amorphous or crystalline layer, depending on the applied voltage, time of process or the type of post-treatment [44–46]. Among the parameters influencing the quality, properties and morphology of the obtained oxide layers, the following can be distinguished: chemical composition of the electrolyte used, process temperature, oxidation time, value of the applied voltage, type of substrate and/or current density (Fig. 2).

The oxidation process undergoes in an electrochemical cell, usually in a three-electrode configuration, in which the anode is a titanium material, the cathode is most often platinum, and the reference electrode can be a saturated calomel electrode. In order to form an oxide layer, it is necessary to diffuse ions from the metal into the layer being formed. The applied electric field allows to overcome the energy barrier that activates this process, which in turn leads to the formation of an oxide layer on the anode surface. The coating has a high resistivity compared to the electrolyte and metal parts of the circuit. Nevertheless, the growth of the oxide layer will be visible

as long as the applied electric field is strong enough to pass ions through the formed oxide layer [34,46,47]. In general, about 100 V for TiO_2, a breakdown of the dielectric occurs (this value varies depending on the chemical compositions of electrolyte used and other process parameters) [34,46,47]. This is the origin of the micro-arc oxidation method where higher voltages are applied [7,48] and it is described in detail herein in Chapter 3.

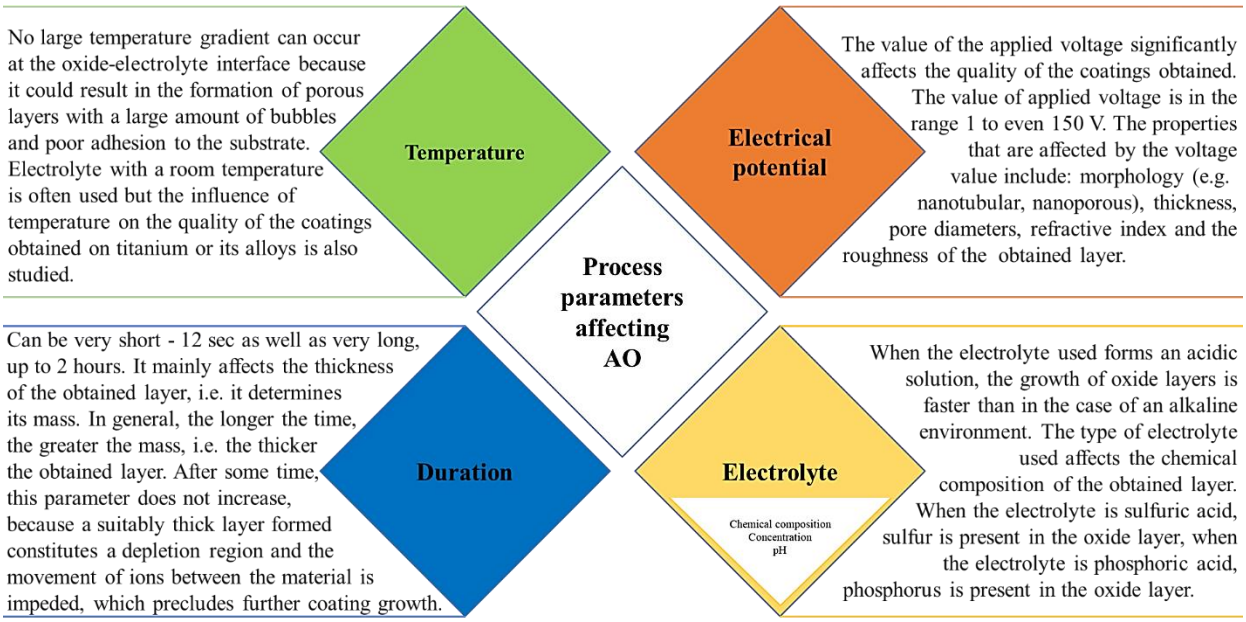

Fig. 2 Most often modified process parameters affecting anodic oxidation and their influence on the coating [21,22,28,37,39,40,46,47,49–55]. Designed and illustrated by the authors of the present work.

2.1. Properties of coating in anodic oxidation

2.1.1. Morphology of coating in anodic oxidation

Anodic oxidation enables the production of titanium alloy coatings with promising application properties in biomedicine. Due to the possibility of varying various parameters, solid and porous coatings can be obtained. Porous coatings in particular seem to be future-proof, as they more closely resemble the bone structure and may allow for the transport of drugs [34,44,46]. Analysing the literature [21,54,56,57] it can be stated, that the porosity of the coating can be increased by increasing the electrolyte concentration, electrolyte temperature, process duration as well as increasing the electrical voltage. For example, the effect of changing the electrolyte composition on the morphology of the oxide layers on the Ti-6Al-4V titanium alloy is shown in Fig. 3. Nonetheless, the size and distribution of anode oxide pores on titanium alloys depend on the structure of the substrate. For instance, it was noted that the nanotubes obtained over the α phase on the Ti-6Al-4V alloy were characterized by thinner walls and larger internal diameters in relation to the nanotubes over the β phase [21]. This may be due to faster dissolution in the vanadium-enriched β phase than in the α phase [58]. The individual conditions of the oxidation process on titanium and its various alloys and the morphology of the obtained coatings shows Table 1.

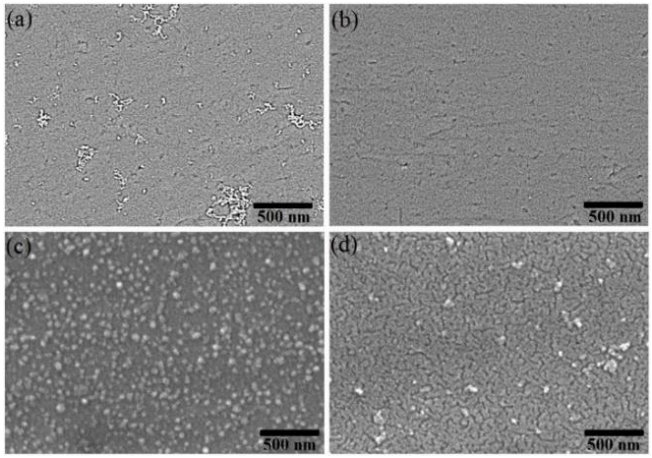

Fig. 3 SEM micrographs of coatings applied on Ti-6Al-4V, subjected to AO treatment at a voltage of 30 V as a function of Na_2SO_4 concentration (a) 0 M, (b) 0.5 M, (c) 1.0 M, and (d) 1.5 M. More particulars associated with morphology are detailed in Table 1. Reprinted from [59], with permission from Elsevier (license number 5420341216939).

Table 1 The individual conditions of the oxidation process on titanium and its various alloys and the morphology/structure/crystallinity of the obtained layers

Material	Electrolyte	Parameters				Morphology/Structure/Crystallinity	Kind of post-treatment and structure after post-treatment	References
		Temperature	Time	Voltage	Current			
CP-Ti	1 M H_2SO_4 and 0.08 M HF	5, 10, 25, 30, 50 and 70 °C 25 °C	12 sec to 1 h 1 h	-	≈5 – ≈45 mA/cm^2	TiO_2 tunneling nanotube	-	[53]
CP-Ti (99.5% Ti)	Glycol-based solutions with 0.3 M NH_4F and 2 wt% of deionized water addition Glycerol-based solutions with 0.3 M NH_4F and 2 wt% of deionized water addition	40 °C	1 h	50 V	-	Nanoporous/nanotubular morphology	-	[22]
CP-Ti (tioblast)	1 wt% HF and 1 M CH_3COOH	Room temperature	20 min	2 – 25 V	-	5 V - nano-pits > 10 V nanopores > 20 self-organized nanotubes	Annealing; 300 – 450 °C anatase + rutile > 550 °C rutile	[40]
CP-Ti (Grade 2)	0.5 wt% NH_4F and 5 vol% deionized water into $C_2H_6O_2$	< 30 °C	1 h	20, 40, 60, 80 and 100 V	0.02 A	20 – 100 V nanotube TiO_2 structure and titanium phases	Heat treatment at 450 °C for 1 h; anatase and rutile	[57]
CP-Ti (Grade 4)	Aqueous solution 1.5 M of H_3PO_4 with $Ca(CH_3CO_2)_2$ or $K(C_2H_3O_2)$ at different concentration of 0.5, 1 and 1.5 M	Room temperature	1 min	Max 150 V	Max 0.5 A	Anodic porous titania	-	[50]
CP-Ti (Grade 4)	98 vol% $C_2H_6O_2$ and 2 vol% distilled water	-	30 min	60 V	-	Nanoporous rods – amorphous TiO_2	-	[30]
CP-Ti (Grade 4)	1 mol/L NH_4SO_2 and 0.15 mol/L NH_4F solution	-	2 h	30 V	-	Nonregular nanopores	-	[60]
Pure Ti	1M NaF solution	Room temperature	1 h	10 V	-	Layer of uniform and homogeneous nanotube arrays	-	[52]
Pure Ti	Aqueous solution $6H_8O_7$ (50 mg/mL) + graphene oxide	25 ± 2 °C	1 h	0, 10, 30, 50, 70 and 90 V	-	Anatase	-	[61]

Material	Electrolyte	Parameters				Morphology/Structure/Crystallinity	Kind of post-treatment and structure after post-treatment	References
		Temperature	Time	Voltage	Current			
Pure Ti	1 M H_2SO_4 solution	-	1 min	70 V	-	3-dimensional network structure; a lot of pores; anatase and rutile	-	[38,56]
Pure Ti	0.5 wt% HF solution	-	-	20 V	-	Titanium oxide nanotubes	-	[24,54]
	1.5 M H_2SO_4+ 0.3 M H_3PO_4+ 0.3 M H_2O_2 mixture solution	-	-	70 V	-			
Ti-6Al-4V	1.2 M NaOH solution	-	2 min	30 V	-	Rutile and sodium titanate ($Na_2Ti_6O_{11}$) with poor crystallinity	-	[38]
	1.35 M NaOH solution						-	
	1.5M NaOH solution						-	
Ti-6Al-4V	$C_2H_6O_2$ solution containing 0.5 wt% NH_4F and 2.5 vol% deionized water	Room temperature	30 min	20, 40, 60, 80 and 100 V	-	20 V – no porous layer 40 V – porous compact layer 60 V - remnants of this porous compact layer and the presence of defined nanotubular structures 80, 100 V – well-defined nanotubes	-	[21]
			60 min			20, 40 V – remnants of this porous compact layer the presence of defined nanotubular structures 60 V, 80, 100 V – well-defined nanotubes		
			120 min			20 V – remnants of this porous compact layer and the presence of defined nanotubular structures 40, 60 V – well-defined nanotubes 80, 100 V – nanograss		
Ti-6Al-4V	Diluted H_2SO_4	-	2 min	10-90 V	-	<20 V amorphous oxide layer >80 V crystalline oxide layer (anatase + rutile)	-	[62]
Ti-6Al-4V	1.5 mol/L H_2SO_4 solution	25 °C	10 min	100 V	-	Nanoporous anatase-TiO_2 structure and small diffractions of rutile	-	[31]
Ti-6Al-4V	1 M H_2SO_4 and 0.08 M HF	5, 10, 25, 30, 50 and 70 °C	12 sec to 1 h	-	≈5 – ≈45 mA/cm^2	TiO_2 tunneling nanotube	-	[53]
		25 °C	1 h					
Ti-6Al-4V	1 wt% HF and 1 M CH_3COOH	Room temperature	20 min	2 – 25 V	-	5 V – nano-pits > 10 V nanopores > 20 self-organized nanotubes	Annealing; 300 – 450 °C anatase + rutile > 550 °C rutile	[40]

Material	Electrolyte	Parameters				Morphology/Structure/Crystallinity	Kind of post-treatment and structure after post-treatment	References
		Temperature	Time	Voltage	Current			
Ti-6Al-4V	Na_2SO_4 (0.1, 0.5, 1.0 or 1.5 M) with 0.2 M $(CH_3COO)_2Ca \cdot H_2O$ and 0.04 M $C_3H_7CaO_6P \cdot 5H_2O$	-	-	30 V	-	Anatase (more anatase was formed on the surface of Ti-6Al-4V substrate with a higher concentration of Na_2SO_4) < 0.5 M Na_2SO_4 – flat structure 0.5 M Na_2SO_4 – some pores 1.0 M Na_2SO_4 – the surface particulate or nodular 1.5 M Na_2SO_4 – the particulate or nodular appearance lost (the high dissolution rate of the anodic oxide surface)	-	[59]
Ti-6Al-4V Prepared by Selective Laser Melting	Electrolyte of $C_2H_6O_2$ contains 0.25 wt% NH_4F and 2.0 wt% deionized water	Room temperature	1 h	20 V	-	The uniform nanotubes	-	[51]
Ti-6Al-7Nb	1 M H_2SO_4 and 0.08 M HF	5, 10, 25, 30, 50 and 70 °C 25 °C	12 sec to 1 h 1 h	-	≈5 – ≈45 mA/cm^2	TiO_2 tunneling nanotube	-	[53]
Ti-25Nb-25Ta	$C_2H_4(OH)_2$ + 5 wt% of deionized water + 0.5 wt% of NH_4F	Room temperature	1 h	60 V	-	Nanotube matrix	-	[39]
Ti-13Nb-13Zr	1 M H_2SO_4 and 0.08 M HF	5, 10, 25, 30, 50 and 70 °C	12 sec to 1 h	-	≈5 – ≈45 mA/cm^2	TiO_2 tunneling nanotube	-	[53]
Ti-24Nb-4Zr-8Sn	1 mol/L NH_4SO_2 and 0.15 mol/L NH_4F solution	-	2 h	30 V	-	Nanotube structures. Surface uneven, part of the nanotubes raised, part of the nanotubes sunk.	-	[60]
Ti-10Mo-8Nb	$C_3H_8O_3$ and deionized water (1:1) with the addition of 2.7 wt% of NH_4F	Room temperature	10.8 ks	20 V	-	Amorphous nanoporous layer	Annealing; > 400 °C – anatase > 550 °C – anatase + rutile	[28]
Ti-10V-2Fe-3Al	15 g/L $C_4H_6O_5$	25 ± 3 °C	1 h	-	8 A/dm^2	Amorphous TiO_2 + anatase	-	[49]

2.1.2. Thickness of coating in anodic oxidation

The oxide layer obtained by anodizing shows different properties depending on its thickness. The thickness of the oxide layer can be from tens of nanometres [37] to even tens of micrometres [38]. The optimal thickness of the film for biomedical application has not yet been clearly defined [63]. Nevertheless, it must be thick enough to provide adequate corrosion protection and simultaneously thin enough not to promote delamination of the coating [64].

The process parameters are significant factors influencing the thickness of the coating. As the electrical voltage and / or electrolyte concentration increase, the layer thickness also increases [37,65]. This can also be confirmed for nanotube layers, which are often formed during electrochemical oxidation. For those obtained on Ti-6Al-4V, it is suggested that the increase in tunneling nanotubes (TNTs) occurs proportionally to the applied potential, with a growth factor fg ≈ 1-5 nm/V [25]. Researches conducted by Mallaiah et al. [62] and by Durdu et al. [57] confirmed that thickness increases to a certain value in the quantity of voltage applied as a function of time. The longer the process time, the more mass is deposited on the surface, which results in a thicker layer [53]. However, this coating does not augment ad infinitum, eventually the process inhibits and ultimately stops, as explained in Fig. 2.

The applied voltage influences the obtained thickness of the oxide layer, while the electrolyte used determines the rate of growth of the oxide layer, which is the resultant of the rate of reaction of the formation of the oxide layer and the rate of dissolution of the oxidation products. Summarizing, the thickness of the anodized layer largely depends on the environment in which the process is carried out, the applied voltage and the process time.

2.1.3. Crystallinity of coating in anodic oxidation

Depending on the given conditions of the oxidation process, two types of coatings can be obtained: amorphous or crystalline [66]. The use of low voltages during the anodizing process creates an amorphous layer, while higher voltages - a crystalline layer [62]. TiO_2 exists in three crystalline polymorphs: tetragonal rutile and anatase, and orthorhombic brookite [66,67]. Anatase is formed on titanium and its alloys with the use of lower electrical voltages, while rutile and / or anatase with higher potentials [38,49,62]. The crystallinity of the coating is also influenced by the concentration of the electrolyte used. When the electrolyte concentration is very low, an amorphous coating is obtained. As the concentration increases, it is transformed into a crystalline form - anatase, and then rutile [37]. Ngyyen et al. [59] confirmed this relationship by observing that more anatase TiO_2 was formed on the surface of Ti-6Al-4V substrate with a higher concentration of Na_2SO_4.

Obtaining rutile (or a mixture of rutile and anatase) is crucial as it causes increased proliferation and differentiation of cells such as osteoblasts. In the case of anatase, the number of cells decreases in numbers immediately after they begin to grow on the anatase surface [68]. These differences are due to the fact that rutile is chemically stable, has a simple structure, and greater hydrophilicity that promotes cell attachment to the surface (see section 2.1.8 herein for more details). On the other hand, anatase has a large surface area with numerous OH-groups. Probably the intensive generation of radicals and oxidation cause the decomposition of organic components of cells, thus inhibiting their growth [68–70]. More differences affecting the bioactivity of anatase and rutile can be seen in Fig. 4.

Anatase and brookite are meta-stable and convert to rutile above temperatures of 800-900 °C [66]. Therefore, some scientists use post-treatment after anodizing, to realize this effect. For instance, Louarn et al. [40] applied annealing after anodizing of the CP-Ti and the Ti-6Al-4V in 1 wt% hydrofluoric acid and 1 M acetic acid. After heat treatment at temperatures of 300 - 450 °C, anatase and rutile were obtained, and at temperatures above 550 °C, rutile was reached. A similar relationship is noted in [28], where Ti-10Mo-8Nb was first oxidized in glycerol and deionized water (1: 1) with the addition of 2.7% in NH_4F and then annealed at temperatures of 400-650 °C. Table 1 shows the individual conditions of the oxidation process on titanium and its various alloys and the crystallinity of the obtained layers. A mixture of anatase and rutile should be achieved, which positively influences cell proliferation, and thus accelerates the process of osseointegration of the implant with the tissue.

2.1.4. Chemical composition of coating in anodic oxidation

Anodic oxidation facilitates adjustment of the chemical composition of the coating by changing the chemical composition of the electrolyte or substances dissolved in the electrolyte. This is especially important as the appropriate composition of the scaffold can improve the tribological and mechanical properties of the implant, accelerate the osseointegration of the implant with the tissue and / or impart antimicrobial and immunomodulatory properties [50,71]. Marenzi et al. [50] have used anodic oxidation with the aqueous solution of 1.5 M of H_3PO_4 with $Ca(CH_3CO_2)_2$ or ($K(C_2H_3O_2)$ at different concentration of 0.5, 1 and 1.5 M to obtain a coating on a pure Ti. Anodic porous titania (APT) with the uniform, homogeneous incorporated elements of P, O, Ca or K (from the electrolyte) and Ti (from the substrate), which was examined with EDS, was obtained. The presence of calcium or magnesium titanates, as well as phosphorus oxides in the scaffold may positively spill over into osseointegration, causing rapid and strong interaction of the implant with the bone through biochemical bonding [29,71]. In [61]

aqueous solution of $C_6H_8O_7$ containing reduced graphene oxide (RGO) is used. The anodic oxide film is mainly composed of anatase TiO_2 and a small amount of carbon oxides. Adding RGO to citric acid accelerates the growth rate of oxide barrier layer and reduces applied voltage. Such results may allow for optimization of the process and reduction of its costs. By selecting the appropriate type of environment in which the anodizing processes are carried out, layers with a specific, expected chemical composition can be obtained.

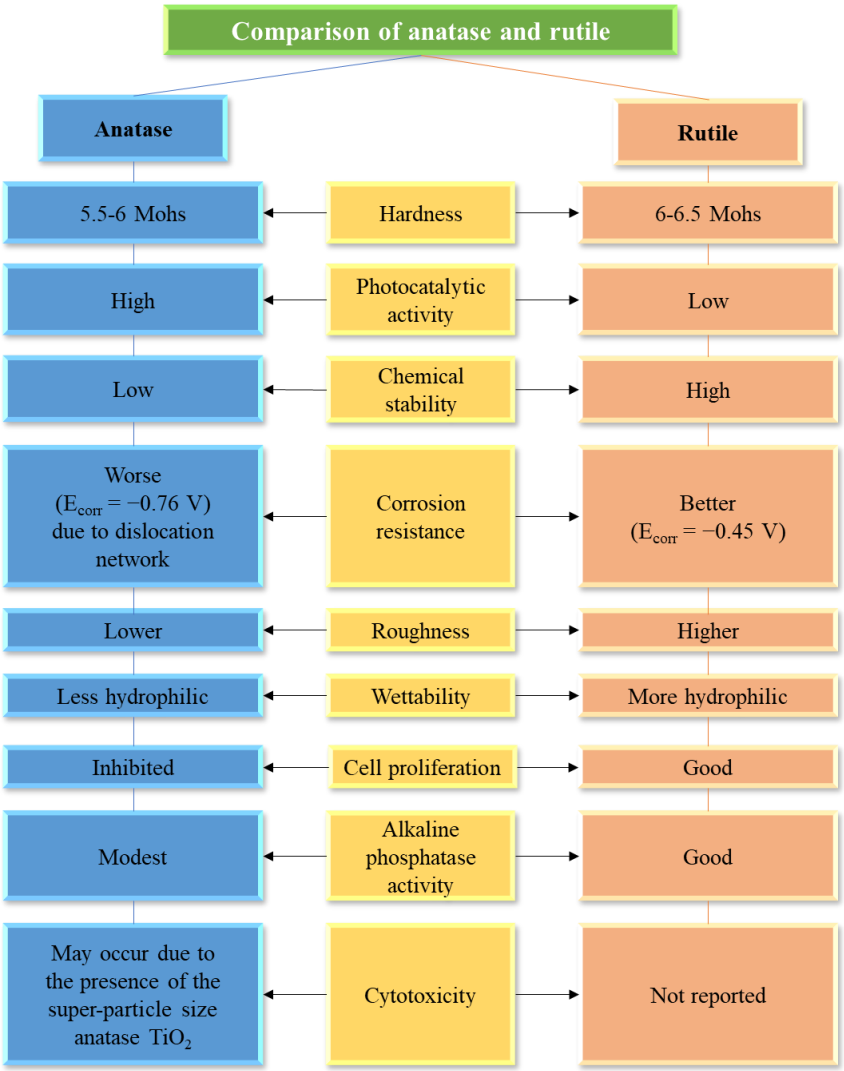

Fig. 4 Comparison of anatase and rutile with regard to their potential use in biomedical applications [68–70,72,73]. Designed and illustrated by the authors of the present work.

2.1.5. Roughness of coating in anodic oxidation

Roughness is a significant factor describing the implant coating. Orthopaedic and dental implants should have a roughness that allows for a permanent connection between the tissue and the biomaterial. Its optimal value supports the proliferation and differentiation of cells because roughness affects the wettability of the surface [63,74]. Most often, as the roughness increases, the hydrophilic nature of the coating increases [69]. The optimal roughness value of the coating for biomedical application, despite many studies, is still unknown. This value should have a positive effect on the increase in cell initiation during osseointegration as well as primary stability [63]. In addition, depending on the surface roughness, it affects macrophage polarization and, consequently, the inflammation process [75].

The roughness of coatings on titanium and its alloys obtained by anodic oxidation ranges from a few nanometres [62] to tens of thousands of nanometres [51]. The roughness values are influenced by the process parameters and the concentration of the electrolyte used. In general, roughness increases with an increase in the applied electrical voltage [57]. The chemical composition of the solution can also modify the roughness of the coating. For example, the roughness of anodic oxide films grown on Ti-6Al-4V substrate decreases with the increased concentration of Na_2SO_4 [59]. The roughness of the anodized layer affects the osseointegration processes, the highest roughness values are generally sought.

2.1.6. Mechanical properties of coating in anodic oxidation

A properly selected set of mechanical properties should ensure the correct cooperation of the implant-tissue-body fluids system. In an aggressive physiological environment, implants are subject to the simultaneous action of corrosive, tribological and fatigue processes, which additionally makes it difficult to achieve the goals. Accordingly, many mechanical properties such as tensile strength, fatigue strength, yield point, elongation, modulus of elasticity and hardness should be determined for the materials used for implants (Fig. 5) [44,76,77]. The last two are the most frequently examined. Pereira et al. [39] have obtained nanotube matrix on the Ti-25Nb-25Ta which hardness was 0.7 ± 0.1 GPa and elastic modulus >12 GPa. Nanoindentation test showed that the hardness and elastic modulus profiles increased with depth. Above the discontinuity at 50 mN, the hardness reached 1.8 ± 0.1 GPa and the elastic modulus remained constant in about 40 GPa. In general, the values of these parameters decreased with increasing voltage. Young's modulus is the basic parameter proving the suitability of a given material for implants and should be as close as possible to the Young's modulus of bone, which is about 10 - 40 GPa and depends on the type of bone and direction (longitudinal or transverse) [78]. It can be concluded that the processing parameters proposed in [39,57] seem to be promising for biomedical application. The average bone hardness is around 30-50 HV and it is intricate to obtain optimal results for the coatings because this parameter is related to elastic and plastic deformations [79,80]. Nevertheless, frequently the hardness of coated biomaterials is higher than that of the uncoated material [37,39,57]. For example, porous oxide coating obtained on Ti-6Al-4V in various concentrations of sulfuric acid solution and different voltages has increased over 300% (from 360 HV for the non-anodized sample to 1116 HV for the anodized sample) [37], which is not an optimal value. The hardness and Young's modulus of the coatings correlate in some way, so their proper adjustment is complicated, but the possibility of changing the parameters of the anodizing process allows for obtaining fruitful results that will be used in biomedicine.

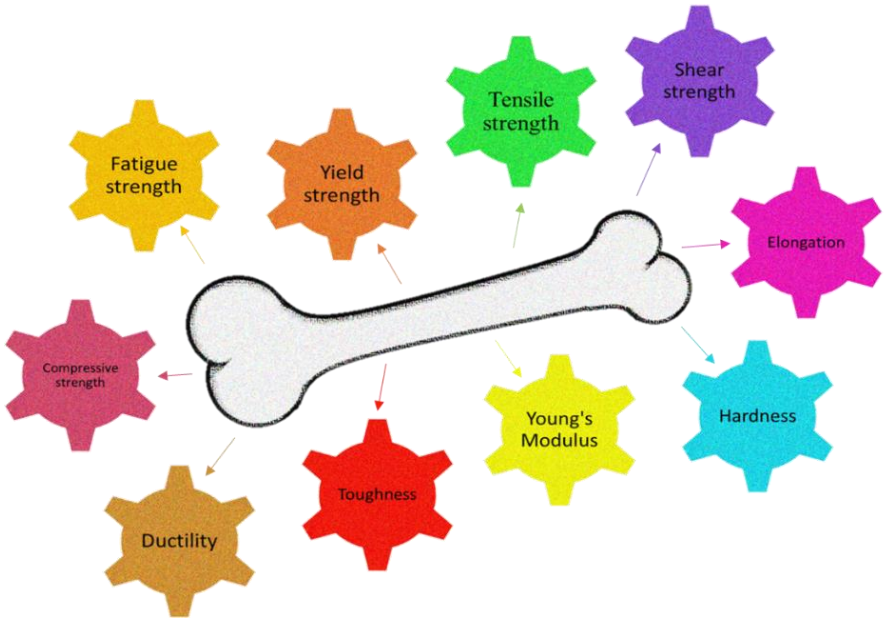

Fig. 5 Mechanical properties of an implant biomaterial [44,76]. Designed and illustrated by the authors of the present work.

2.1.7. Corrosion resistance of coating in anodic oxidation

Corrosion resistance in the case of biomaterials is particularly important because inflammation at the site of implantation can initiate corrosion processes that damage the materials. This process can consequently cause metallosis and loosening of the implant [81]. The appropriate corrosion resistance of metal alloys can be obtained by modifying their chemical properties, and thus changing the microstructure. Titanium and its alloys, in terms of corrosion resistance, have similar properties, which results from the fact that the passive layer formed on their surface has essentially the same nature, i.e. it is formed by titanium oxide or TiO_2 [44,47,82,83]. Liu et al. [49] obtained an amorphous TiO_2 + anatase coating in 15 g/L of $C_4H_6O_5$ on Ti-10V-2Fe-3Al. Coated Ti alloy possessed remarkably improved anti-corrosion performance which was additionally enhanced by LDHs sealing. A similar issue is considered in [61] where the samples anodized at 10–50 V exhibited excellent corrosion resistances. As speculated by the authors, compared with the uncoated substrate of CP-Ti, the corrosion current density of the coated Ti alloy at 50 V was decreased by about 94%, such that the corrosion potential experienced an increase of ≈61%. Samples anodized at 70-90 V display worse corrosion resistance than those anodized at 10-50 V (Fig. 6) which is probably related to the different growth rate of the oxide barrier layer. The goal of scientists is to create

structures that are resistant to bioelectrochemical corrosion and additionally have appropriate biomechanical properties [61,76,82].

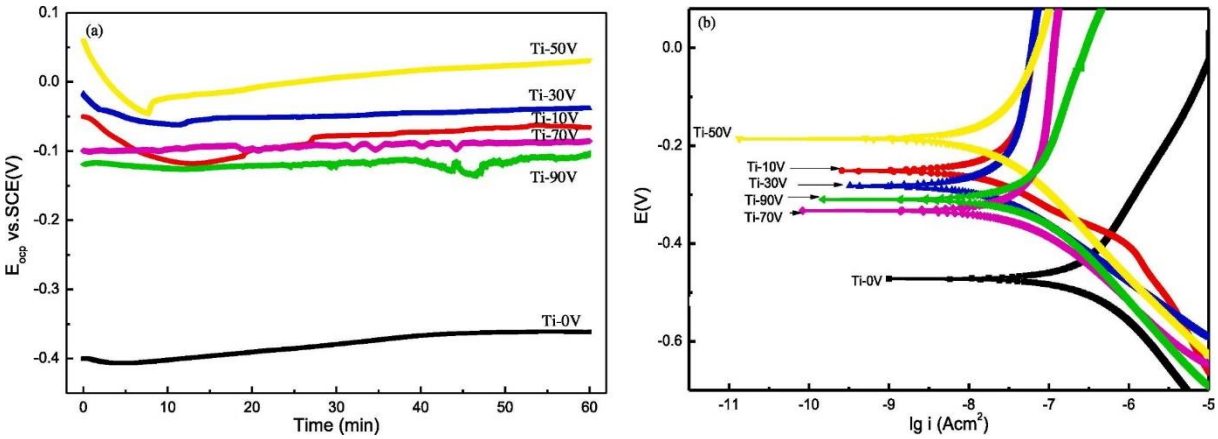

Fig. 6 (a) Open circuit potential curves of the ground and anodized pure Ti samples at different voltages; (b) polarization curves of the ground and anodized pure Ti samples at different voltages. More details about process parameters are specified in Table 1. Reprinted from [61], with permission from Elsevier (license number 5420341338261).

2.1.8. Wettability of coating in anodic oxidation

The wettability of the surface is a physicochemical parameter that determines the quality of the material and its possible use as a biomaterial. In the case of bone implant materials, it is significant that they exhibit a moderate degree of hydrophilicity [84]. Then the adhesion of cells to the surface is stronger, and their proliferation and differentiation is faster [30,31,60]. In addition, a large number of bacteria (including *Staphylococcus aureus*, which is often identified in orthopaedic infections) prefer to abut to hydrophobic surfaces. Therefore, generating the hydrophilic surface can reduce the adhesion of bacteria and thus prevent the occurrence of inflammation [84]. This can be explained by the fact that fimbriae or pili that subsist on the bacterial envelope are hydrophobic in nature, so bacterium will preferentially attach to a hydrophobic surface [84,85].

Thanks to the possibility of changing the oxidation parameters, it is possible to meet these requirements. For example, the contact angle increases from 42.3° to 67.6° with increasing concentration of Na_2SO_4 from 0 M to 1.5 M, respectively [59]. In this case, the greater contact angle induced easier and faster HAp coating formation. This was due to the fact that the about of calcium (which was also present in the electrolyte) in the coating increased with increasing Na_2SO_4 concentration. The presence of Ca improves the formation of apatite and concurrently activates the hydrophobic interaction near the calcium particle, which increases the contact angle [86]. The wettability of the anodized coating varies also from oxidation time. The non-treated sample possessed the most expatiatory contact angle (67.2° ± 1°), and the sample anodized over 60 min displayed the lowest value equalled 15.9° ± 1° [25]. The duration of the process often influences the presence of the various phases of the coating. The use of a shorter time frequently results in the formation of an amorphous coating and its elongation with a crystalline one [25,87]. Moreover, the probable presence of hydrophilic groups reduced the value of the contact angle [87]. This enables the cells to adhere more optimally [88]. The above example shows that the surface of titanium and its alloys can become hydrophilic by anodic oxidation, resulting in a significant increase in the ability of the surface to engage in cell differentiation and proliferation. Thus, the test of the wettability of coatings is one of the basic tests that is performed before *in-vivo* and *in-vitro* assays are carried out [28,40,57]. It is known that the best value for the contact angle to attach cells to the implant is 55° [89,90], while the most desirable contact angle value for hard tissue regeneration is 35° to 80° [89,90].

2.1.9. Surface free energy of coating in anodic oxidation

The surface free energy is another feature of the coating that is related to the biological response of the implant [91,92]. It is not possible to measure it directly. The measurement of the contact angle is used for this, and the quantitative result is obtained indirectly - with the utilization of computer modelling and with use of various approaches [93,94]. The determination of the surface free energy is important because it states the adhesion between the implant and the aqueous phase, i.e. the body fluids in the human body [91]. In other words, it affects the interaction of proteins and the differentiation of osteoblasts, which are responsible for promoting the appropriate implant-tissue interface [95]. This may be explained by the fact that when proteins or cells are located in close proximity to the implant, their surface domains try to align to achieve the lowest possible value of the total free energy of this combination [94,95].

The possibility of changing the parameters of anodic oxidation enables to change the surface free energy. Obtained by Pérez-Jorge et al. [96] nanoporous oxide film (oxidation time 5 minutes) and nanotubular oxide film

(oxidation time 60 minutes) on a Ti-6Al-4V titanium alloy using an electrolyte containing 1M H_2SO_4 and 0.15 wt% HF exhibited different values of surface free energy. To determine them, a contact angle was measured and then a Fowkes approach was used. Nanoporous oxide film had surface free energy of 72.5 mJ/m^2 and nanotubular oxide film of 80.0 mJ/m^2. Different surface morphologies show different surface free energies. It is said that a more complex surface occasions a better connection between the implant and human tissue [34,97]. In addition, the authors investigated the effects of the chemical composition of solution on surface free energy of coating. The presence of fluoride in the coating increased surface free energy. Similar results were obtained in [98]. However, it is worth to emphasize that fluorine compounds possess low value of surface energy [99]. Therefore, it is possible that not only the presence of various chemical compounds may change the values of surface free energy, but also the surface roughness [98]. Moreover, surface free energy and roughness may have a synergistic influence on cell proliferation [100].

2.2. In-vitro assays of coating in anodic oxidation

In-vitro tests are an excellent way to initially determine the behaviour of living cells in the presence of a biomaterial. Their main disadvantage is the fact that they do not give real environmental conditions occurring in a human body. Nevertheless, they open the floodgates of the determination of the biocompatibility of the material. They are relatively cheap and allow to obtain preliminary results of the reaction of cells to the material in a short time [52,101]. The *in-vitro* studies of cells in [28] concerned the development of adipose tissue-derived stem cells after 1 and 7 days on the uncoated surface of Ti-10Mo-8Nb alloy and after anodic oxidation treatment, during which a nanoporous coating was obtained. After 1 day of culture, a slight improvement in the results for the anodized surface was obtained. After 7 days of culture, a slight increase in cell number, mitochondrial activity, and scattering over the uncoated surface was reported. It is worth emphasizing that smooth surfaces (in this case non-anodized) favour cell differentiation [102]. However, cells on such a substrate are often less elongated and overlap, which adversely affects their adhesion to the coating and ultimately the possibility of using the material as an implant [103]. The duration influences the morphology of the coatings and thus the viability of the cells. The issue was investigated by Torres-Avila et al. [25]. Samples anodized with mixture of ethylene glycol, 1 wt% of distilled water and 0.5 wt% of NH_4F were reported to increase or maintain metabolic activity (reading cell growth using the MTT proliferation assay with human fetal osteoblastic cell line), compared to for uncoated Ti-6Al-4V alloy. The maximum metabolic activity, indicating cell viability and proliferation, was observed in the anodized sample for 60 min (three-fold change in metabolic activity 14 days after culture). This was associated with the formation of more hydrophilic coatings with increasing time, which promotes cell adhesion and differentiation [88]. Expansion of cells after anodizing is often observed [30,52]. The increase in the number of cells on biomaterials during *in-vitro* evaluation indicates the possibility of their potential use in implantology [101].

The crucial objective of the biomaterial surface modifications is the increase in their bioactivity, biocompatibility, adhesion, and proliferation of osteogenic cells at a simultaneous limitation of bacterial adhesion and growth at the interface between implant and tissues. The attachment of bacteria on surfaces is affected by the electrostatic double layer, hydrophobicity, roughness, and various other factors [104–106]. Bacteria need to overcome the energy barriers to reach the negative energy regions, thereby facilitating the bacterial attachment [107,108].

2.3. In-vivo assays of coating in anodic oxidation

Positive results of tests carried out during *in-vitro* assays allow for the referral of a given biomaterial to *in-vivo* evaluation [74]. In the first stage, they involve implanting a biomaterial sample under the skin or directly into a specific organ of a laboratory animal. In the next stages (at the stage of clinical trials), the biomaterial is implanted in a selected group of people [109,110]. *In-vivo* assays in the rat model examined by Li et al. [52] show that the anodized surface of the CP-Ti with layer of uniform and homogeneous nanotube arrays promotes osseointegration and exhibit a higher bone bond strength compared to the CP-Ti substrate which is not coated. The presence of nanotubes increases hydrophilicity and promotes an increase in cell adhesion, which has a positive effect on osseointegration *in-vivo* [87,88,111]. Another model – a rabbit femur model was used in [40]. Histological analysis after 4 weeks showed direct apposition of bone to the surface of biomaterial. The porous structure created by anodizing increases the contact between the implant and the tissue, thus improving their biomechanical interlocking and ensuring greater bond strength. Obtaining such results is very promising and will probably facilitate the use of the obtained coated biomaterials for preclinical trials [109,110].

Overall, anodic oxidation typically allows one to adjust the properties of coatings in broad aspects (morphology, thickness, crystallinity, chemical composition, roughness, mechanical properties, corrosion resistance, surface wettability). Due to possibility of adjusting the process parameters (mainly voltage, current, deposition time and chemical composition of the solution), it is likely to conform the above-mentioned properties of the coatings. It should be noted that the change of one process parameter does not necessarily result in a linear increase/decrease of all properties of the coatings. Moreover, alteration of the electrolyte composition can result

in the formation of various structures (nanotubes, nanopores, nanocrystals), which can be unforeseeable. Therefore, process optimization is extremely complicated. Nevertheless, the aforementioned tests and their analysis are necessary in order to further evaluate the coatings in terms of biological properties (first *in*-vitro and then *in-vivo* analysis) and their possible application in implantology. It is worth mentioning that in the case of anodic oxidation, the improvement of biological properties is often associated with additional thermal treatment to obtain rutile and anatase, which show better biocompatibility. Nevertheless, the analysis of the presented papers allows one to conclude that 'oxidation and possibly additional thermal treatment allow the production of coatings on titanium and its alloys with relatively good biomechanical and anti-corrosion properties and have the potential for applications beyond the laboratory scale'.

3. Micro-arc oxidation

Plasma electrolytic discharge dates back to around 1880, when Sluginov described this phenomenon. In the meantime, attempts were made to accurately describe them and use them in industrial practice, but it only happened in the 1970s. It was during this period that the method of producing ceramic coatings on an aluminum substrate was described using the plasma electrolytic discharge, which was minor contribution to its further development. It was called anodic spark deposition (ASD). Only about 30-40 years ago, research and their activities led to the deployment of the method in the first practical applications, and its present-day name is micro-arc oxidation [112].

Micro-arc oxidation (MAO) is a novel method that facilitates to generate oxide-ceramics coating on the metal surface as Ti, Al, Mg, Zn, Nb, Be, Ta, Hf, Fe, Zr and their alloys as well as on brass and c-graphite materials [7,33,112,113]. Another name for this process is anodic spark oxidation (ASO) [114], plasma electrolytic oxidation (PEO), anodic spark deposition (ASD), plasma chemical oxidation (PCO), anodic oxidation by spark discharge (ANOF) [112] or plasma electrochemical surface ceramic coating [115]. MAO can be considered as developed method of anodic oxidation, as it is quite similar. As with anodizing, the following parameters can be changed when using the MAO method for depositing coatings: electrolyte temperature and composition, deposition time, voltage, current density and so on [7]. A significant difference between these two methods is the value of the applied voltage during MAO, because it is much higher and must be above the breakdown limit of the formed oxides [7,33,112]. According to the Ikonopisov electron avalanche breakdown model, this value depends on many variables of the electrolyte - its composition, concentration and resistance [116]. However, it was assumed that this value for TiO_2 is about 100 V, and the MAO process for titanium and its alloys is often carried out at a voltage above 150 V [7]. Visible micro-discharges on the substrate or audible cracking often occurs during the MAO process, resulting in more porous and less uniform oxide layers compared to anodized coatings [7,114,116]. Unfortunately, the detailed mechanism of the formation of coatings during the MAO process has not yet been investigated [117].

3.1. Process parameters in micro-arc oxidation

Carrying out the MAO process on titanium and its alloys can lead to obtaining hard, porous coatings with good corrosion and wear properties, hence it is becoming more and more popular in biomedical applications [7,112,114]. The properties of the coatings depend on many variables: electrolyte composition, voltage, current density, duration, as well as pre- and post-treatments (Fig. 7) [117,118].

The composition of the electrolyte directly affects the composition of the coating obtained on the surface of the material. For example, when MAO was executed on TNZ in a mixture of 3.20 mol/dm^3 $Cu(NO_3)_2$ in H_3PO_4 at 450±10 V, a porous coating which contained copper (3.7 ± 0.4 wt%) and phosphorus (18.5 ± 0.3 wt%) was obtained [119]. Performing the process in an aqueous electrolyte solution with 0.08 mol/dm^3 $C_3H_7Na_2O_6P{\cdot}5H_2O$ and 0.8 mol/dm^3 $(CH_3COO)_2Ca{\cdot}H_2O$ on Ti-3Zr-2Sn-3Mo-25Nb resulted in the formation of the coating which included Ca and P as well as Ti and O [120]. The composition of the electrolyte also influences the morphology, porosity, thickness and corrosion resistance of the coatings. This is because the composition and concentration of the electrolyte affect the sparking voltage [117]. Alteration in the composition and concentration of the electrolyte appeal to the film obtained using the MAO process, what will be described in detail in later sections.

The voltage used is one of the most important process factors. Due to the fact that it is high (for titanium and its alloys it is most often above 150 V), sparks appear on the surface of the material, which affect the morphology, thickness and crystallinity of the coating [112]. The voltage used to deposit coatings on titanium and its alloys is usually from 200 V [33] to 500 V [121], however, voltages of as much as 650 V are used either [122].

Current density is another parameter that acts upon the morphology, surface roughness, corrosion resistance and composition of the coating deposited on titanium or its alloys [123]. The most common is a constant current density mode, because with the passage of time in the process, the intensity of the spark discharge increases and the number of spark discharges decreases. As a result, it is possible to obtain coatings with large micro-pores. The use of variable current density during MAO is also used. Particularly important is the case of reducing

the current density over time, as it reduces the intensity of the spark discharge, which will contribute to the formation of a more homogeneous and less porous coating [117].

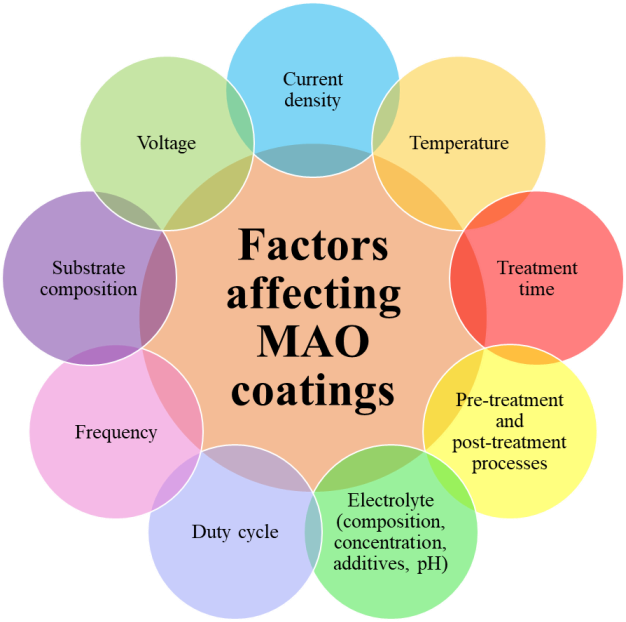

Fig. 7 Factors affecting plasma electrolytic oxidation coatings for biomedical applications [117,118,124]. Designed and illustrated by the authors of the present work.

The duration of the MAO process is key variable that affects the coating. In general, increasing the oxidation time increases the size of the micropores, decreases the number of micropores, and increases the thickness of the coating [125]. The exact influence of time on the quality of the obtained coatings is described in subsequent subsections.

Before the actual processing, a given material may undergo many processes, called pre-treatment processes, aimed at improving the properties of the final coating [117]. Among them can be distinguished:

- electropolishing which can affect the chemical composition of the passive layer formed after this treatment, as well as better the roughness and corrosion resistance of the MAO coating [126,127]
- magnetoelectropolishing (where the magnetic field is applied through electropolishing) that enables one to determine the morphology of the MAO coating; pore sizes impose impact on the corrosive and mechanical properties of the final coating [60,119,127–129]
- particle shot-peening which allows to increase fatigue life and adjust the roughness of the substrate thanks to which it is possible to control the roughness of the MAO coating [121,128,130]
- sandblasting, the application of which determines the original morphology of the MAO coating as well as may alter its chemical composition and mechanical properties [55,130,131]
- pre-anodizing which facilitates refinement of the density of the inner part of the MAO coating, and thus increases its corrosion resistance. It does not significantly affect the morphology and chemical composition of the coating [132,133].

Post-treatment processes are aimed at changing mainly the morphology, chemical composition and crystallinity of the obtained coating [112,117]. Thermal and hydrothermal treatments are mainly used [134].

3.2. Properties of coating in micro-arc oxidation

3.2.1. Morphology of coating in micro-arc oxidation

The surface morphology has a direct influence on the bioactivity of the coating [135,136]. Fortunately, it can be shaped depending on the parameters used during process. One of the most crucial variables weighing the surface morphology is the applied voltage. As the final voltage enhances, the porosity of the coating originally increases, and after reaching a certain value it tends to decrease [137]. The influence of changes in the voltage and duration of treatment on the morphology of the coating obtained on the Ti-13Nb-13Zr was investigated in [33]. The mean pore diameter has been reported to vary from 1.8 to 8.4 µm with increasing voltage (200-400 V). For the highest voltage (400 V), reducing the time (from 15 min to 10 min) under the same current conditions (32 mA) reduces the pore size, while increasing the current intensity (50 mA) increases the pore size. Similar observations were noticed by Wei et al. [138] while depositing the coating on Ti-6Al-4V. Once the voltage increases (200-450 V), the average size of the micropores increases, and thus the number of the coating micropores decreases (Fig. 8). This dependency is probably due to the connecting of some discharge channels, resulting in a larger vacancy [33]. Another relationship can be obtained when changing the frequency of pulses. In the tests carried out on Ti-6Al-

4V by Sobolev et al. [41], a symmetrical bipolar square pulse with a frequency of 200 to 1000 Hz was used. It was noticed that the change of the pulse frequency influences the size of the pores obtained. As the frequency of the current increases, the size of the pores decreases and their number increases. In [139], the porosity of the coatings decreased with increasing frequency. This is because the use of higher frequencies results in more discharges per unit area [139,140]. On the other hand, the size of micropores and microcracks slightly increased with increasing pulse width and single pulse energy [125] what is also associated with the change in discharges. Altering the chemical composition of the electrolyte causes modifications in morphology. It results from [141] that an increase in the concentration of K_2SiO_3 in the solution caused an increase in the diameter and number of pores of coating on Ti-13Nb-13Zr. Of course, the treatment time also influences the morphology of the coatings. Many researchers confirm that as the MAO time increases, the size of the micropores increases and their number decreases [122,125,135,142]. This is due to the fact that as the time increases, micro-discharges are formed in the pores that have shaped before, which is caused by the dielectric breakdown [125,143]. The ability to modify the surface morphology as well as the size and number of micropores is crucial in the case of implants. MAO has a wide range of variable possibilities, thanks to which it is possible to obtain an optimal porous structure. This is particularly important as the appropriate porous titanium coatings induce the formation of a tissue-implant interface without the need for additional osteogenic cells or osteoinductive agents [144].

Table 2 shows the individual conditions of the micro-arc oxidation process on titanium and its various alloys and the morphology/structure of the obtained layers. The analysis shows that the parameters of the MAO process, especially the voltage, electrolyte composition, pulse width and single pulse energy, have an important influence on the size and diameter of micropores and microcracks.

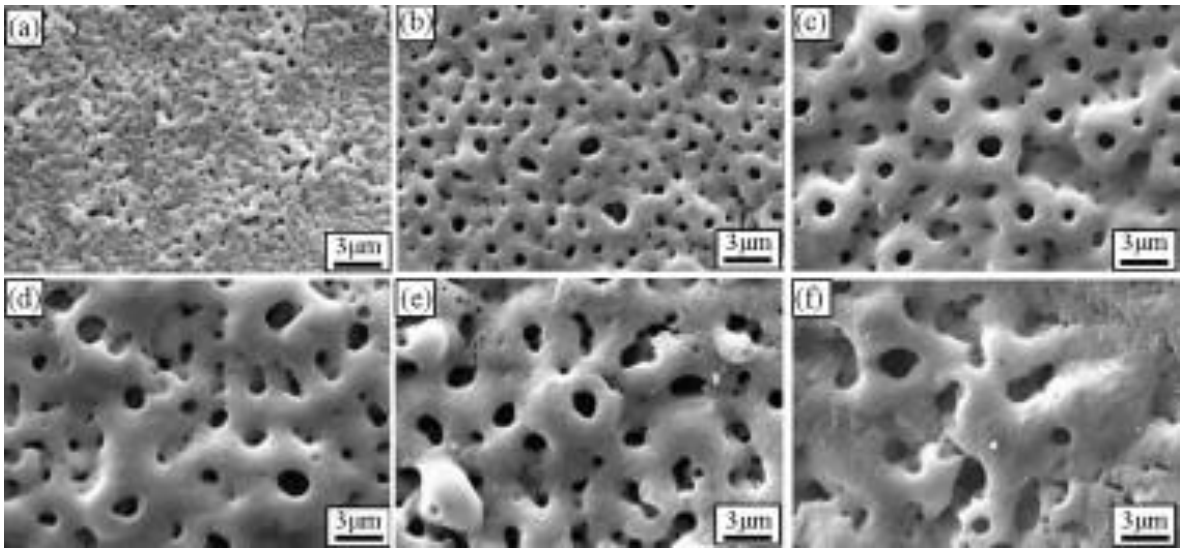

Fig. 8 SEM images of the MAO coatings applied on Ti-6Al-4V treated at a different voltages: (a) 200 V, (b) 255 V, (c) 300 V, (d) 350 V, (e) 400 V and (f) 450 V. More specifics attributable to the morphology are detailed in Table 2. Reprinted from [138], with permission from Elsevier (license number 5420341489313).

3.2.2. Thickness of coating in micro-arc oxidation

The dependence of the coating thickness on the processing parameters is similar for each of the described electrochemical methods. In the case of MAO, the thickness of the coatings increases (to a certain value) with increasing voltage either [33,125,126,138]. However, in the case of an increase in voltage in the constant current density mode, the coating increases its thickness, but to a much lesser extent than in the case of an increase in the current density in the constant voltage mode [122]. This should be emphasized that as the width of the electric pulse increases, the energy of a single pulse increases, which also increases the thickness of the coating [145]. This is because enhancement the energy expands the film formation rate, which ultimately translates into a greater thickness. On the other hand, the thickness of the coating decreases with increasing frequency (200 Hz - 2 μm, 1000 Hz - 1 μm) [41] and with increasing temperature (−3 °C - 13.6 ± 0.8 μm, 20 °C - 10.8 ± 0.4 μm) [146]. Sowa et al. [126] reported that the lower the concentration of electrolyte additives, the thinner the coating. Similarly, with the increase in HA concentration in the electrolyte, the thickness of the coatings increases [147]. During the MAO process, micro-discharges form in the coating, creating pores that allow particles to enter from the electrolyte. A higher concentration of electrolyte causes an intensified filling with ions, which increases its thickness [148]. It is generally accepted that the bond strength between the substrate and the oxide layer is more beneficial with increasing coating thickness [125]. This is important because the implant coating in the human body should not crack, delaminate or detach from the substrate [117].

Table 2 The individual conditions of the micro-arc oxidation process on titanium and its various alloys and the morphology/structure/crystallinity of the obtained layer

Material	Electrolyte	Parameters				Morphology/Structure/Crystallinity	References
		Temperature	Time	Voltage	Current		
CP-Ti	Solution of 20 g/L $Na_3PO_4 \cdot 12\ H_2O$	20 ± 1 °C	-	470 V	-	Biomimetic coatings with pores. The addition of calcium acetate caused an increase in porosity and a decrease in the average pore size. Both coatings with the presence of rutile and anatase. Confirmed the presence of perovskite, HAp and amorphous calcium phosphates on the second coating.	[149]
	Solution of 20 g/L $Na_3PO_4 \cdot 12\ H_2O$ + 25 g/L $Ca(CH_3COO)_2$						
CP-Ti (Grade 2)	Solution of 0.014 M $Na_2SiO_3 \cdot 5H_2O$, 0.20 M $C_4H_6O_4Ca$, 0.50 M $NaNO_3$, 0.0010 M $C_3H_7Na_2O_6P$, 0.025 M $Na_2EDTA \cdot 2H_2O$	23.0 ± 1.5 °C	7 min	500 V	-	Irregular and complex coating with facets with nonuniform aggregates and craters with circular pits. Peaks of amorphous Ti as well as crystalline phases (anatase and rutile) were observed.	[150]
Pure Ti	Phosphate sodium solution (10 g/L)	< 20 °C	5 min	450 V	-	Typical porous morphology with pores of an average size of ~1.2 μm. Confirmed presence mainly of α-titanium and anatase.	[151]
	Phosphate sodium solution (10 g/L) and SiO_2 nanoparticles (8 mg/mL)					Porous coating with uniform incorporated SiO_2 nanoparticles into the MAO coating. Confirmed presence mainly of α-titanium and anatase - no effect of SiO_2 incorporation on the formation of crystalline phases.	
Pure Ti (99.9% Ti)	Solution of $Na_2SiO_3 \cdot 9H_2O$ (10 g/L), $(HOCH_2CH_2)_3N$ (5 mL/L) and HCl (1 mol/L)	< 40 °C	10 min	50 V	-	Smooth and crack-free surface with not uniformly distributed diminutive pores. Prevalence of titanium, rutile and a low amount of silica.	[136]
Ti-6Al-4V	Aqueous electrolyte solution with 10 g/dm^3 Na_2CO_3 and 2 g/dm^3 $Na_2SiO_3 \cdot 5H_2O$	30 °C	15 min	250 V	0.05 A/cm^2	Sample surface with numerous micro and submicron pores. Presence of the titanium phase and two phases of titanium oxide - rutile and anatase.	[41]
Ti-6Al-4V	Aqueous electrolyte solution with 10 g/dm^3 $NaAlO_2$, 5 g/dm^3 Na_3PO_4, 0.5 g/dm^3 Na_2EDTA and 0.05 mL/dm^3 $C_3H_8O_3$	20 – 40 °C	-	440 – 470 V	-	Coatings with evenly distributed micropores. They mainly contain rutile, anatase and a large amount of Al_2TiO_5.	[145]
Ti-6Al-4V	Aqueous electrolyte solution with 0.025 mol/dm^3 $Ca(CH_3COO)_2 \cdot H_2O$, 0.075 mol/dm^3 $Ca(H_2PO_4)_2 \cdot H_2O$ and 0.045 mol/dm^3 NaOH	-	-	500 V	-	Porous coating mainly with anatase, rutile and a small amount of amorphous phase (calcium phosphate)	[121]
Ti-6Al-4V	Solution of 0.1 M $Ca(CH_3COO)_2 \cdot H_2O$, 0.05 M $C_3H_7CaO_6P \cdot H_2O$, 0.15 M $C_{10}H_{18}N_2Na_2O_{10}$ and 20 g/L NaOH	–3 °C	20 min	290 V	0.2 A/cm^2	Porous and rough coatings. For –3 °C a coating with a large number of closed micropores (open-porosities: 4.8 ± 0.2%), for 20 °C a coating with open micropores (open-porosities: 8.1 ± 0.5%). The presence of anatase and rutile. Decreasing the temperature increases the intensity of the rutile peak and descends the anatase peak, as well as reduces the intensity of the peaks originating from the substrate.	[146]
		20 °C					

Material	Electrolyte	Parameters				Morphology/Structure/Crystallinity	References
		Temperature	Time	Voltage	Current		
Ti-6Al-4V	Solution of $Na_2SiO_3 \cdot 9H_2O$ (10 g/L), $(HOCH_2CH_2)_3N$ (5 mL/L) and HCl (1 mol/L)	< 40 °C	10 min	50 V	-	Granular structure with pores. Occurrence of titanium, rutile and a modest amount of silica	[136]
Ti-6Al-4V	Aqueous electrolyte solution with $(CH_3COO)_2Ca$ and $C_3H_5(OH_2)PO_4Ca$	< 30 °C	1, 5, 10, 20, 40, 60 or 120 min	-	0.123 A/cm^2	Porous and rough coatings. 5 - 120 min: crystalline phases based on HAp and calcium apatite (secondary structures). Crystallinity increased with increasing processing time	[125]
Ti-6Al-4V	Aqueous electrolyte solution with 6.3 g/dm^3 $Ca(CH_3COO)_2 \cdot H_2O$, 13.2 g/dm^3 $Ca(H_2PO_4)_2 \cdot H_2O$, 15.0 g/dm^3 EDTA-2Na and 15.0 g/dm^3 NaOH	40 °C	5 min	-	8 A/dm^2	200 V - low intensity anatase; homogeneous coating 250-300 V - pronounced anatase and amorphous calcium phosphate; the surface of the coating relatively regular and porous 300-400 V - pronounced anatase and amorphous calcium phosphate; rough, irregular and porous coating 450 V - anatase, rutile and amorphous calcium phosphate; rough, irregular and porous coating	[138]
Ti-6Al-4V	Aqueous electrolyte solution with 0.2 M $(CH_3COO)_2Ca$, 0.1 M $NaH_2PO_4 \cdot 2H_2O$ and $C_6H_9O_6Y \cdot xH_2O$ (0.0 g/L, 1.0 g/L, 1.5 g/L or 2.0 g/L)	25 °C	10 min	380 V	-	The morphologies of the Y-doped and undoped coatings are similar. Volcano-like structures formed on their surfaces. Rutile and anatase are mainly detectable in all coatings. No influence of yttrium addition on the phase composition of TiO_2 coatings. Yttrium not detected by XRD.	[152]
Ti-6Al-4V	Aqueous electrolyte solution with 0.12 M Na_3PO_4 and HAp (0.0 g/L, 1.0 g/L, 1.5 g/L or 2.0 g/L)	< 35 °C	5 min	300 V	0.5 A/dm^2	Porous coatings (the porosity decreased with increasing HAp concentration). 0 g/L of HAp - only Ti and anatase phases. 1.0 g/L - 2.0 g/L of HAp - anatase, HAp and tricalcium phosphate. The increase in HAp concentration in the electrolyte increases the intensity of HAp and TCP reflections.	[147]
Ti-6Al-4V	Solution of $Ca(CH_3COO)_2 \cdot H_2O$ (6.3 g/dm^3), $Ca(H_2PO_4)_2 \cdot H_2O$, (13.2 g/dm^3), EDTA-2Na (15 g/dm^3) and NaOH (15 g/dm^3)	40 °C	5 min	230 V	-	Porous coating with the presence of calcium and phosphorus	[55]
Ti-6Al-4V	5 g of Na_3PO_4, 3 g of CaF_2, 2 g of KOH in 1000 mL distilled water	Before process: 23 °C After process: 53 °C	10 min	Max 400 V	1 A	Coating with irregular micropores with different sizes (captured by crimped shape pores). Presence of seven phases: fluorapatite, HAp, tricalcium phosphate, anatase, rutile, aluminium oxide and vanadium (V) oxide.	[153]
Selective Laser Melted Ti-6Al-4V	Aqueous electrolyte solution with 0.1 M $C_4H_6CaO_4 \cdot H_2O$, 0.06 M Na_2HPO_4, and NaOH	-	0.2, 0.5, 1, 5, 10, 15 or 20 min	-	9 A/dm^2	Porous coatings with unevenly distributed pores. Increasing the processing time reduces the number of micropores and simultaneously increases the porosity (more larger pores). Prolonging the duration escalates the intensity of the anatase and rutile diffraction peaks. Presence of peaks from substrate.	[154]

Material	Electrolyte	Parameters				Morphology/Structure/Crystallinity	References
		Temperature	Time	Voltage	Current		
Ti-6Al-7Nb	Aqueous electrolyte solution with 0.252 mol/dm^3 Na_2HPO_4 and 0.115 mol/dm^3 NaH_2PO_4	-	1, 5 or 10 min	240 or 290 V	2.5 - 10 mA/cm^2	All samples are porous. Presence of anatase for each sample. No matrix elements and presence of Na and P (low level).	[135]
Selective Laser Melted Ti-13Zr-13Nb	Aqueous electrolyte solution with 0.1 mol/dm^3 $C_3H_7CaO_6P$ and 0.15 mol/dm^3 $Ca(CH_3COO)_2$	Room temperature	10 or 15 min 10 min	200, 300 or 400 V	32 mA 50 mA	A porous coating with an increasing mean pore diameter from 1.8 to 8.4 μm with increasing tension. Anatase at lower voltages and anatase and rutile at higher voltages.	[33]
Ti-13Nb-13Zr	0.1 M $Ca(H_2PO_2)_2$ solution with additions of $Ca_3(PO_4)_2$, $CaSiO_3$ or SiO_2	-	5 min	350 or 450 V	150 mA/cm^2	All coatings are porous. Presence of mainly anatase and bioactive compounds in coatings.	[155]
Ti-39Nb-6Zr	Aqueous electrolyte solution with 2.5 g/dm^3 KOH	-	10 min	400 V	-	A coating with a large number of submicropores and micropores. No cracks at the interface between the coating and the matrix. A coating with anatase (TiO_2), rutile (TiO_2) and Nb_2O_5 phases as well as monoclinic ZrO_2 and $ZrTiO_4$ phases.	[156]
Ti-3Zr-2Sn-3Mo-25Nb	Aqueous electrolyte solution with 0.08 mol/dm^3 $C_3H_7Na_2O_6P{\cdot}5H_2O$ + 0.8 mol/dm^3 $(CH_3COO)_2Ca{\cdot}H_2O$	< 50 °C	7 min	250, 500 V	-	A porous structure with micron-sized pores, being a mixture of TiO_2 and a small amount of amorphous phase with titanium peaks. TiO_2 present as anatase and rutile, but the intensity of anatase peaks stronger than that of rutile.	[120]
Ti-29Nb-13Ta-4.6Zr	Aqueous electrolyte solution with 0.1 mol/dm^3 $C_3H_7CaO_6P$ and 0.15 mol/dm^3 $C_4H_6MgO_4$	-	8 min	-	12 mA (312 A/m^2)	Thick porous oxide layer with rutile and anatase	[6]
Ti-35Nb-2Ta-3Zr	Solution of $Na_2SiO_3{\cdot}9H_2O$ (10 g/L), $(HOCH_2CH_2)_3N$ (5 mL/L) and HCl (1 mol/L)	< 40 °C	10 min	400 V	-	Rough, porous surface where fine pores are nested in the bigger pores. Micro-cracks are visible. Distribution of anatase, rutile, Nb_2O_5 and $NaNbO_2$ confirmed.	[136]
Ti-15Zr-7.5Mo	Aqueous electrolyte solution with 0.1 mol/dm^3 $C_3H_7CaO_6P$ and 0.15 mol/dm^3 $C_4H_6CaO_4$	-	10 min	400 V	31.2 mA/cm^2	Porous amorphous oxide layer	[9]

3.2.3. Chemical composition of coating in micro-arc oxidation

The appropriate selection of the chemical composition of the coatings is a pivotal task because its optimization often results in the acceleration of the growth of permanent implant-tissue interface. Often, materials that have not been properly treated do not show bioactivity [157]. The chemical composition of the coating is mainly modified by changing the chemical composition of the electrolyte [48,158]. In [126] the deposition of coatings on Ti-13Nb-13Zr was carried out with the use of MAO in an aqueous electrolyte solution with 0.01 mol/dm^3 $Ca(H_2PO_2)_2$, as well as in an aqueous electrolyte solution with 0.1 mol/dm^3 $Ca(H_2PO_2)_2$ and 0.1 mol/dm^3 H_3PO_4. All samples were covered with relatively homogeneous oxide layers containing the substrate elements (Ti, Zr and Nb) and the components of the aqueous electrolyte solution (Ca and P). The addition of phosphoric acid to the electrolyte only slightly increased the amount of P in the coating. An increase in the amount of one of the elements occurs along with its increase in electrolyte concentration [159]. Simka et al. [141] reported that the amount of silicon on the coatings increased with the concentration of K_2SiO_3 in the solution (from aqueous electrolyte solution with 5 g/dm^3 KOH and 0.1 mol/dm^3 K_2SiO_3 to aqueous electrolyte solution with 5 g/dm^3 KOH and 1.0 mol/dm^3 K_2SiO_3). A similar concern was raised in [160] where the dependence of the concentration of H_2SO_4 and H_3PO_4 in the solution was investigated. This is because the concentration of the electrolyte affects the quality and quantity of the discharges by altering the quantity and diameter of the generated pores, thus modifies the probability of ions filling of the pores [141,148]. Another variable that appeals to the chemical composition of the coating is the voltage. In [141] samples treated at 100 V revealed appearance of TiO_2, Nb_2O_5 and ZrO_2, but silicon was not detected. For the samples at 200 V, the presence of oxygen and silicon was found, which could indicate the formation of SiO_2. For the voltage of 400 V, the presence of a significant amount of silicates which the Si/O atomic ratio equals 0.46 or 0.50 was confirmed in the coatings. There was also a high concentration of potassium. This is also due to the change in micro-discharges with increasing voltage. The influence of the applied current frequency on the chemical composition of the coatings was investigated in [41], where the coating was deposited on the Ti-6Al-4V alloy in an aqueous electrolyte solution with 10 g/dm^3 Na_2CO_3 and 2 g/dm^3 $Na_2SiO_3 \cdot 5H_2O$. The investigations confirmed the presence of Ti, Al and V (from the matrix) as well as Si and Na (from the electrolyte). The chemical composition of all samples was almost the same and did not depend significantly on the current frequency used (from 200 to 1000 Hz). As can be seen, the process parameters can significantly act upon the composition of the coatings obtained in the MAO process. However, it is mainly transformed by altering the composition of the electrolyte. As a result of this, it is possible to intercorporate elements with different properties into the coatings (Fig. 9). Most often, in order to obtain a biocompatible coating on titanium and its alloys, calcium and phosphorus compounds are used [33,125,126,140,161], which ions in the MAO process form a hydroxyapatite phase on the coating. This phase possesses biocompatible and bioactive properties, supporting osseointegration of the implant with human tissue [161,162]. In addition, the chemical compounds to the solutions used in the MAO process include, inter alia, the following:

- molybdenum, which improves the electrochemical stability of the coating, thereby increasing its corrosion resistance [163,164]
- silver showing high antibacterial properties (however silver nanoparticles have been reported to be toxic) [42,43,113]
- zinc, which also has excellent antibacterial properties and is essential in a variety of biological processes, including bone biomineralization [113]
- copper as an anti-bacterial factor in coating [113]
- magnesium, which promotes calcium deposition and also regulates cell proliferation [165].

Moreover, many scientists in their research attempt to incorporate several components simultaneously, such as strontium and silicon [43], magnesium and zinc [166], zinc and silicon [167], magnesium, manganese, silicon, strontium and zinc [168] molybdenum and silicon [164], graphene nanosheets and nanoHAp [169] and even polymers [170]. Such activities are aimed at creating coatings with the best properties, adapted to the human body. The range of chemical compounds used in this area is tremendous.

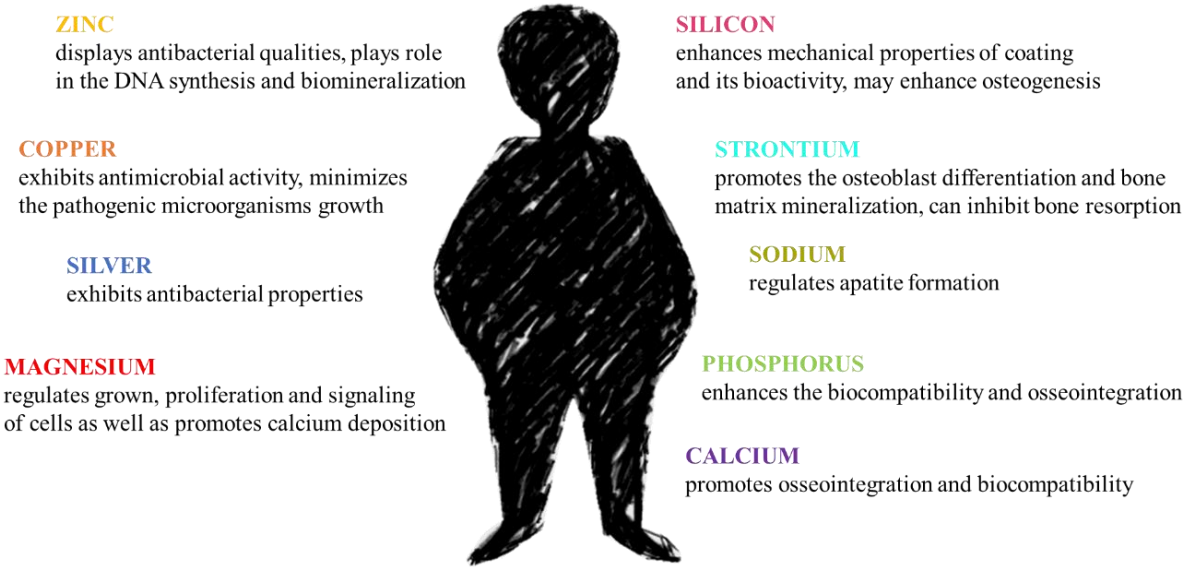

Fig. 9 Elements incorporated in MAO coatings on titanium implants and their effect on the human body [41,43,51,73,113,140,165,167,171,172]. Designed and illustrated by the authors of the present work.

3.2.4. Crystallinity of coating in micro-arc oxidation

The crystallinity of the coating is an extremely important parameter, especially in biomedical applications. As mentioned, titanium dioxide exists in various crystallographic forms [67]. In the case of implantology, crystalline phases have exceptional properties, because they favour osseointegration to a significant extent (compared to amorphous phases) [173]. In general, anatase occurs at lower voltages, while a mixture of anatase and rutile or rutile appears at higher voltages [33]. This dependence is confirmed by Wei et al. [138] who deposited the coating on Ti-6Al-4V. They noticed that at low voltage (200 V) the diffraction reflex of anatase transforms into rutile at higher temperatures with enhancing dielectric breakdown [33]. Moreover, in this study, for the coatings above 250 V, an amorphous baseline appeared, the intensity of which increased with the increase of the applied voltage. It may be assigned to the amorphous phase of calcium phosphate (CaP) [33,174]. In [41], the process was carried out at 250 V, but the frequency of the current was changed in the range from 200 to 1000 Hz. The coatings had a titanium phase as well as rutile and anatase. With the increase in the treatment frequency, the content of the anatase phase decreased and the rutile phase content increased at the same time. This may have been due to the transformation of anatase into rutile when the process reached the dielectric breakdown temperature [41,66]. The MAO process carried out by Kazek-Kesik et al. [155] on Ti-13Nb-13Zr in 0.1 M $Ca(H_2PO_2)_2$ solution with additions of $Ca_3(PO_4)_2$, $CaSiO_3$ or SiO_2 at 350 V and 450 V resulted in the formation of coatings consisting mainly of anatase and not rutile. Despite the applied high voltage, the transformation of anatase into rutile probably did not occur because, as mentioned, the breakdown value of the oxides also depends on the composition, intensity and resistance of the electrolyte, which is consistent with the Ikonopisov electron avalanche breakdown model [124]. However, it is worth noting that these researches confirmed the presence of bioactive compounds in coatings (mainly calcium and phosphorus, which are part of hydroxyapatite [162]). The presence of HAp in the coatings was confirmed by researchers in [125]. The process was carried out in an aqueous solution of electrolyte made of acetate $(CH_3COO)_2Ca$ and calcium glycerophosphate β-$C_3H_5(OH_2)PO_4Ca$ for 1 - 120 min. Crystalline phases based on hydroxyapatite and calcium apatite have been reported to form in the coatings over 5 minutes. The crystallinity of these phases increased with increasing processing time. The highest amount of amorphous HAp was obtained for the coating produced in 5 min, and the highest amount of crystalline hydroxyapatite phase was obtained for the coating produced in 120 min. This is coherent with the fact that the thickness of the layer increases with time, which in turn intensifies the micro-discharges that result from the dielectric breakdown, thereby increasing the temperature and changing the crystallinity [125,143]. The influence of electrolyte composition at 400 V was investigated by Karbowniczek et al. [12]. The coating obtained with the use of an aqueous electrolyte solution with 7 g/dm^3 Na_2HPO_4 and 20 g/dm^3 $C_4H_6O_4Ca{\cdot}H_2O$ had crystalline phases: hydroxyapatite, rutile and anatase, as well as $CaTiO_3$. The coating deposited in an aqueous electrolyte solution with 7 g/dm^3 $C_3H_9O_6P$ and 20 g/dm^3 $C_4H_6O_4Ca{\cdot}H2O$ did not have a hydroxyapatite phase and was mainly amorphous, although the presence of anatase, rutile and $CaTiO_3$ was confirmed. On the other hand, for the aqueous electrolyte solution with 7 g/dm^3 Na_2HPO_4 and 20 g/dm^3 $C_3H_7CaO_6P{\cdot}H_2O$ also no HAp phase was observed, and the coating was mainly amorphous, although anatase and rutile were present. This is because the composition of the electrolyte affects the sparking voltage, so as the composition changes, it changes the breakdown value of the dielectric [34,46,47].

Table 2 shows the individual conditions of the micro-arc oxidation process on titanium and its various alloys and the crystallinity of the obtained layers.

3.2.5. Roughness of coating in micro-arc oxidation

Despite recent developments in the field of biomaterials, the optimal value of implant surface roughness for osseointegration is still ambiguous [63,149]. However, experience has shown that an appropriate increase in surface roughness promotes bone adhesion directly to the implant surface and minimizes the risk of fibrous layer formation [175]. The micro-arc oxidation process causes an increase in surface roughness, which is confirmed by various studies [126,141,156]. In general, the surface roughness of the coatings increases with increasing voltage applied during the process [121,155]. It is worth emphasizing that this increase is not linear. For example, in [141] during the MAO process on Ti-13Nb-13Zr in an aqueous electrolyte solution with 5 g/dm^3 KOH and 0.1 mol/dm^3 K_2SiO_3, an increase in coating roughness was observed for all deposition voltages (compared to uncoated Ti-13Nb-13Zr). However, at 100 and 200 V, the increase was slight. On the other hand, at a voltage of 400 V, a significant increase in roughness was noticed (from 0.15 μm to 5.54 μm). This may be because a change in the voltage value changes the number and size of the micropores, which is directly related to the roughness of the coating [33]. Sowa et al. [126] noted that for coatings obtained under constant voltage (400 V), the surface roughness increased with the concentration of the electrolyte solution. A similar relationship was observed in [15], where the roughness of coatings on Ti-6Al-4V increased with increasing HAp concentration in the electrolyte [147]. By increasing the concentration of the electrolyte, more ions fill the pores and thus the surface roughness increases [141,148]. High roughness and surface development can promote a good bond between the implant and the tissue. An improvement in properties for roughness Ra = 0.39–1.6 μm is noted [173]. However, other properties such as morphology, crystallinity, chemical composition, etc. also influence osseointegration [67,149,173].

3.2.6. Mechanical properties of coating in micro-arc oxidation

Metals, including titanium and its alloys, are widely used in hard tissue engineering because they exhibit very good mechanical properties that are sufficient to withstand the stresses that arise during the use of the implant. Nevertheless, various types of treatments (e.g. micro-arc oxidation) are often used to increase the mechanical strength of the material, such as hardness and wear resistance [30,176]. Young's modulus is one of the basic parameters characterized during the researches [78,84]. The research carried out in [33] confirms that the use of MAO with an aqueous electrolyte solution with 0.1 mol/dm^3 $C_3H_7CaO_6P$ an 0.15 mol/dm^3 $Ca(CH_3COO)_2$ on Ti-13Zr-13Nb at 200 - 400 V changes the Young's modulus. The values of the modulus of elasticity for all MAO coatings were closer to the bone values, with the best value obtained for a voltage of 400 V. A decrease in the value of this parameter was also observed in [177]. Formation of a porous structure on the surface of the titanium alloy could cause reduction of the Young's modulus of the material [178]. The surface hardness after MAO treatment in most cases increases [156]. For example, in [179] the Vicker's hardness increased from $HV_{0.05}$ 323 ± 16 to $HV_{0.05}$ 712 ± 58. It is presumed that the increase in microhardness is due to the formation of crystalline anatase and rutile. It is worth emphasizing that the hardness of the coating is largely influenced by the composition of the electrolyte. Lederer et al. [139] reported that the addition of zirconia nanoparticles to the electrolyte increased the hardness of the coating to an average value of 12.8 GPa [compared to the untreated sample (4.1 GPa) and PEO samples without the addition of nanoparticles (8.5 GPa)]. According to the [180] addition of Al_2O_3 and ZrO_2, there is no significant improvement hardness of MAO coatings. Different hardness values in [181] were detected, where the coatings produced in aluminate-phosphate electrolytes and in silicate and aluminate-silicate solutions were investigated. The former showed the Knoop microhardness of 575 kg/mm^2, the latter 305-375 kg/mm^2. The composition of the electrolyte influences the hardness of the coating mainly because it changes the sparking voltage, changing the crystallinity of the coating [34,46,47]. Moreover, the composition of the electrolyte also influences the adhesion of the coating to the substrate [176]. It is esteemed, that the adhesion strength of the MAO coating to the implant substrate is signally higher than that of traditional coating deposition methods [182]. However, Yerokhin et al. [181] reported that the coatings produced in the silicate and aluminate-silicate solution did not show strong adhesion, while the coatings produced in the aluminate-phosphate electrolytes had a high adhesion value. This is mainly due to the fact that in the silicate electrolyte, the formation of silicate oxides is characterized by an outward growth. Whereas in the phosphate electrolyte it mainly takes place from the oxidation of the substrate and the growth of the oxides inwards [176]. It was reported in [147] that with the increase in HAp concentration in the aqueous electrolyte solution with 0.12 M Na_3PO_4, the coating adhesion strength deteriorated. Also, in [121] it was noted that the fatigue strength of all samples with the MAO coating decreased compared to the alloy without the coating due to the brittleness of the ceramic coatings. Obtaining the appropriate mechanical properties is a complicated issue and requires the selection of many process parameters: voltage, chemical composition of the electrolyte, deposition time, etc. However, obtaining a coating that has optimal properties is crucial in implantology [10,11,183].

3.2.7. Tribological properties of coating in micro-arc oxidation

Titanium and its alloys have poor tribological properties, mainly characterized by a high coefficient of friction, high adhesive wear and low abrasion resistance [184,185]. The spontaneously formed oxide layer on their surface does not guarantee adequate protection of the material in an aggressive environment such as the human body [3,114]. In addition, the use of an implant may result in infections due to the accumulation of the wear debris [184]. In the case of tribological properties, the electrolyte composition [151,176] and the appropriate pre- and post-treatment [118,185] have a particular influence on the quality of coatings. Chen et al. [156] conducted MAO on Ti-39Nb-6Zr in an aqueous electrolyte solution with 2.5 g/dm^3 KOH at 400 V for 10 minutes. In one of the samples the top loose layer of the MAO film was polished by emery paper up to 2000 grade and a dense layer was left. This sample is named as P-MAO. The second sample is MAO, only after micro-arc oxidation treatment. Both coatings were reported to exhibit greater wear resistance than uncoated titanium alloy (under dry friction conditions at ambient temperature, 200 °C and 400 °C). Moreover, the MAO and P-MAO coatings had a low wear indicator at ambient temperature. The polishing of the MAO coating led to a reduction in the wear indicator of the coating at high temperature (compared to the MAO coating without polishing). Post-treatment resulted in a reduction in the coefficient of friction. It should be stresses that both coatings showed mainly adhesive wear, while the uncoated titanium alloy abrasive, adhesive and oxidizing. In [121], coatings on Ti-6Al-4V were produced with the use of micro-arc oxidation and with a combination of two processes: micro-arc oxidation and fine particle shot-peening (FPSP). The wear resistance was reported to be greater for the FPSP-MAO samples compared to the MAO samples. This is probably due to the fact that FSPS reduces the body wear by introducing a "dimple" structure on the surface of the FPSP-MAO coating [121,186]. In the case of coatings formed in different electrolytes, the added chemical compounds are of importance. In [181], the coatings created in the phosphate solution with the use of MAO decreased the friction coefficient. On the other hand, the layers formed in the aluminate-phosphate electrolyte led to an increase in the minimum wear rate of the sample, however, the friction coefficient remained in the range of 0.6–0.7, which was probably caused by the transfer of material from the counterface.

3.2.8. Corrosion resistance of coating in micro-arc oxidation

Titanium is a material that, due to its self-passivation, hardly corrodes in a neutral environment (including solutions containing chloride ions). Titanium alloys have corrosion resistance similar to that of pure metal [3]. Consequently, they are often used in implantology. However, their very good properties deteriorate in the aggressive environment of body fluids. As a result, the treatment is often necessary in order not to cause allergic reactions, which can lead to e.g. the implant loosening [81]. Sobolev et al. [41] reported that the corrosion resistance of the MAO coating formed on Ti-6Al-4V in an aqueous electrolyte solution with 10 g/dm^3 Na_2CO_3 + 2 g/dm^3 $Na_2SiO_3 \cdot 5H_2O$ at 250 V is 40 times greater than that of the uncoated alloy. Moreover, the higher the frequency of the current pulses (from 200 to 1000 Hz), the higher the corrosion resistance of the obtained coating was. This was probably due to the surface morphology, as the higher frequency resulted in a more compact and low porosity oxide coating. Significant improvement in corrosion properties was also observed in [123] and in [187], where the open-circuit potential values of the coated samples were much higher than that of the untreated sample (Fig. 10). For almost all samples (the variable was a voltage of 150–450 V), the polarization resistance also increased (calculated from Tafel slopes from polarization curves – Fig. 11). In addition, no pitting corrosion up to a potential of 3 V was observed and the samples had very good corrosion resistance in Ringer's solution. The influence of the chemical composition of electrolyte on corrosion resistance was investigated in [181]. It was noted that the electrolyte coating with silicates was the most resistant to corrosion in sulfuric acid solution and had the lowest corrosion rate at potentials up to 1.7 V. On the other hand, the electrolyte coatings with phosphates showed better corrosion properties in NaCl solutions and physiological fluids, and also showed relatively low corrosion rates up to 2.0 V (value twice as low as uncoated titanium alloy). Such values are mainly due to the chemical stability of the phases contained in these films and the dense structure of the coating. Anatase, rutile and HAp which are often detected in MAO coatings exhibit good anti-corrosion properties [188].

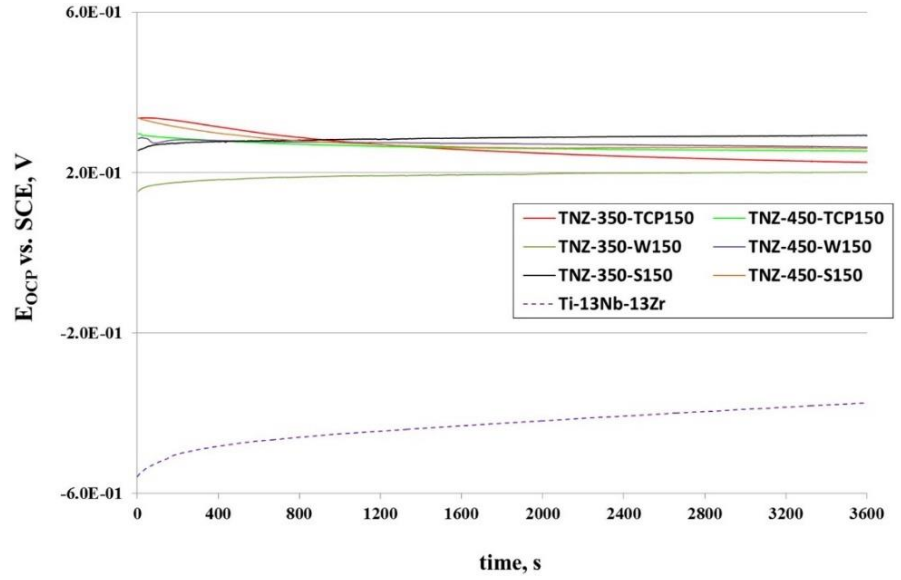

Fig. 10 Open circuit potential curves for the uncoated and micro-arc oxidized Ti-13Nb-13Zr samples at 350 and 450 V on baths with different chemical compositions**.** TNZ-350-TCP150 - bath with 0.1 M $Ca(H_2PO_2)_2$ and 150 g/dm^3 $Ca_3(PO_4)_2$, TNZ-350-W150 - bath with 0.1 M $Ca(H_2PO_2)_2$ and 150 g/dm^3 $CaSiO_3$; TNZ-350-S150 - bath with 0.1 M $Ca(H_2PO_2)_2$ and 150 g/dm^3 SiO_2. Reprinted from [187], with permission from Elsevier (license number 5420350082693).

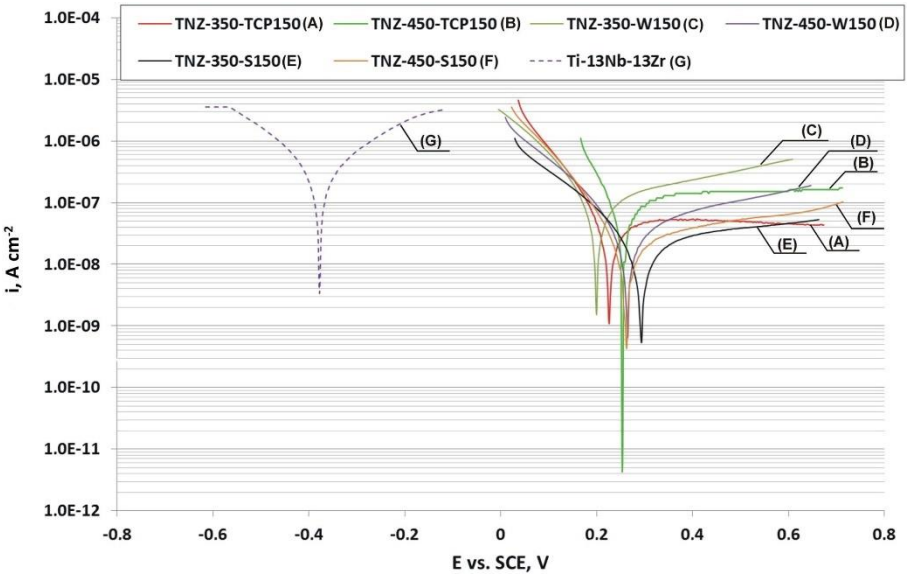

Fig. 11 Polarization curves for the for the uncoated and micro-arc oxidized Ti-13Nb-13Zr samples; legend as in Fig. 10 Reprinted from [187], with permission from Elsevier (license number 5420350082693).

3.2.9. Surface free energy of coating in micro-arc oxidation

Surface free energy is indirectly related to surface wettability and is also responsible for proper cell differentiation and proliferation [95]. The higher the surface free energy, the easier it is for the surface to interact with biological samples [25,91]. Therefore, it is necessary to determine the surface free energy of the MAO coating. Echeveryy-Rendon et al. [189] investigated the influence of various parameters of the MAO process on the properties of the coating on the CP-Ti (Grade 2) and Ti-6Al-4V titanium alloys deposited in an electrolyte containing H_3PO_4 and H_2SO_4. In order to determine the value of the surface free energy, the contact angle was measured 22 days after the MAO process, and then the Neuman method was used. It was noted that higher surface energy occurs in those coatings where both anatase and rutile occurred. On the other hand, for the sample, of which coating was composed only of anatase (the deposition process was shorter and at a lower voltage compared to the above-mentioned samples), this value is lower. It may be due to the thermodynamical nature of these polymorphs of titanium dioxide [190]. Nevertheless, no correlation was found that would allow to determine the exact relationship between the process parameters and the surface free energy of the coating. Takebe et al. [191] investigated CP-Ti (Grade 2) micro-arc oxidized at 350 V in an electrolyte containing 0.01 M β-glycerophosphate and 0.15 M calcium acetate monohydrate. In order to determine the surface free energy, the contact angle was

measured, and then the method of Owens was used. The lowest value was obtained for CP-Ti, a much higher value for CP-Ti after the MAO process, and the highest value for CP-Ti after the MAO process and hydrothermal heating with high-pressure steam at 300 °C. This is probably due to changes in the surface morphology that occurred after the heat treatment. The more complex surface of titanium implants can lead to better bonding at the implant-tissue interface [34,97].

3.3. Inducing apatite films – immersion tests after micro-arc oxidation

An important type of *in-vitro* test to check the bioactivity of the scrubbed coatings is the simulated body fluid (SBF) immersion test, which reflects the aggressive nature of the human organism's environment. It is because the SBF solution in its composition contains mineral ions in concentrations very similar to the concentration of human blood plasma [153,192]. The consumption of phosphates and calcium ions that are present in the SBF solution should contribute to the unprompted growth of bone-like apatite nuclei on the surface of the coating. Therefore, the formation of apatite on the surface of the biomaterial during the immersion test is considered a successful development of new bioactive coatings [193]. This is due to the fact that during the formation of a permanent connection at the tissue-implant interface, the generation of a bone-like layer of apatite on the surface of the implant plays an important role [113,194,195]. The immersion test consists in soaking samples with coatings formed in the micro-arc oxidation process under appropriate temperature conditions (most often 37 °C) [120], removing the samples after a specified number of days (1, 2, 7, 14, 30 or more days) [4,120,196] and finally submitting the sample to tests such as: SEM, EDS, XRD or others [120]. In [120] the induction of apatite on coatings formed on Ti-3Zr-2Sn-3Mo-25Nb in an aqueous electrolyte solution with 0.08 mol/dm^3 $C_3H_7Na_2O_6P{\cdot}5H_2O$ and 0.8 mol/dm^3 $(CH_3COO)_2Ca{\cdot}H_2O$ was investigated. The study showed that after 7 days of immersion, the samples showed a large amount of white, scale-like particles. However, after 14 days, scaly particles covered the entire porous surface of the samples. XRD examination confirmed the presence of apatite peaks already 7 days after immersion. It can be predicted that apatite was probably formed on the surface of the coatings. Positive results of the bioactivity study were also obtained in [121,177] as well as in in [197] where the surfaces of Ti-6Al-4V and Ti-6Al-7Nb oxidized in an aqueous electrolyte solution with $(CH_3COO)_2Ca{\cdot}H_2O$ and Na_3PO_4 were covered with hydroxyapatite (HAp was not deposited on untreated alloys). The MAO coatings were covered with numerous minor flakes and micron spherical deposits, rich in calcium and phosphorus. In [126], a different apatite induction rate was observed depending on the voltage and concentration of $Ca(H_2PO_2)_2$ in the solution used during the MAO process. For the sample at a voltage of 200 V and in an aqueous electrolyte solution with 1 mol/dm^3 Ca $(H_2PO_2)_2$, after 7 days, crystallites appeared at the pore boundaries, but there was a small amount of them. However, for the sample at a voltage of 400 V and in an aqueous electrolyte solution with 0.1 mol/dm^3 $Ca(H_2PO_2)_2$, the formation of crystallites was observed after 7 days, and after 28 days, they began to transform into clusters. The compound that precipitated out was tricalcium phosphate and crystalline titanium. It was also noted in [155] that the amount of apatite particles on the coating was higher when MAO was performed at a higher voltage (450 V) compared to the process performed at 350 V. However, this trend continued in the first days of the immersion test. After 28 days of the test, apatite crystals covered all surfaces with layers of apatite.

The bioactivity of coatings can also be tested in Hank's solution. The test principle is the same as for the immersion test in SBF. The concentration of ions in such a solution is similar to the concentration of ions in the extracellular fluid. This allows for the initial determination of the bioactivity of the coating in order to activate faster bone regeneration and to remedy the endamaged tissues [48]. Dziaduszewska et al. [33] performed the MAO process on Ti-13Zr-13Nb in an aqueous electrolyte solution with 0.1 mol/dm^3 $C_3H_7CaO_6P$ and 0.15 mol/dm^3 Ca $(CH_3COO)_2$ at 200, 300 and 400 V. The specimens were immersed in the Hank's solution at 37 °C for 72 h. The tests showed that the obtained coatings possessed the ability to form calcium phosphate. The films obtained had a high Ca/P ratio, which indicates a good bioactivity of the coatings. The value of the Ca/P ratio closest to the stoichiometric hydroxyapatite was obtained at a voltage of 300 V. In [6], tests were carried out in Hank's solution without glucose. Ti-29Nb-13Ta-4.6Zr samples after the MAO process in an aqueous electrolyte solution with 0.1 mol / dm^3 $C_3H_7CaO_6P$ and 0.15 mol/dm^3 $C_4H_6MgO_4$ and uncoated samples were tested. After immersion of the samples for 7 days, Ca and P were detected on both the clean sample and the treated TNTZ sample. However, the concentration of Ca and P for the MAO sample increased significantly with the immersion time. The MAO-treated TNTZ was completely covered with a layer about a few micrometres thick, which was made of calcium phosphate, after only about 7 days. Negative results of bioactivity tested in Hank's solution without glucose were obtained by Tsutsumi et al. [9], who deposited a coating on Ti-15Zr-7.5Mo. The immersion test was run for 7 days and the solution was changed after 3 and 5 days. Scientists did not observe any deposit formation on the MAO coating, so no calcium phosphate had formed on the layer. This was probably due to the high amount of Zr in the coating obtained after the MAO process, which reduced the ability to form calcium phosphate. However, it can be seen that the presence of phosphorus and calcium in the electrolyte positively affects the bioactivity of the coatings [113].

3.4. In-vitro assays of coating in micro-arc oxidation

Cell culture systems are responsible for assessing the biocompatibility of implant materials before their introduction to further research (*in-vitro* tests on animals and finally clinical trials on humans). They allow the study of the mechanisms of action during the interaction of the tissue with the implant [113,198]. Consequently, their popularity is growing and the types of cells used for research are diverse (Fig. 12). Lim et al. [55] investigated the biological response to SAOS-2 cells lines. The cell proliferation rate, alkaline phosphatase activity and cell adhesion for the MAO shell formed on Ti-6Al-4V were significantly higher compared to the Ti-6Al-4V samples which were machined and grit-blasted. The SAOS-2 cell lines in the MAO

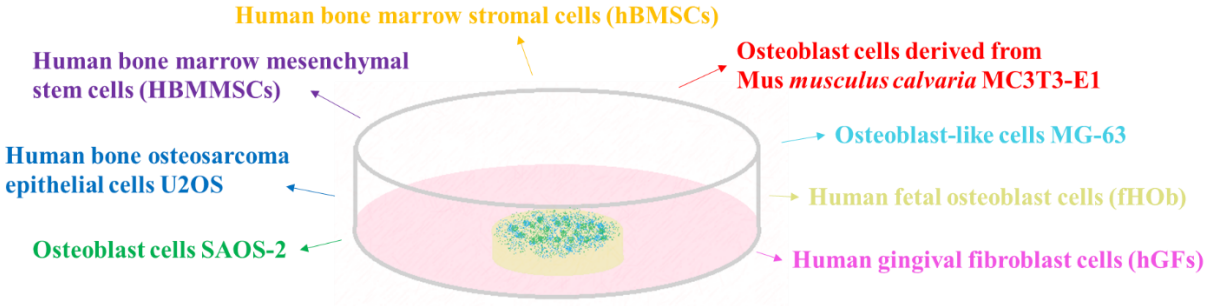

Fig. 12 Types of cell lines used for *in-vitro* assays [55,60,120,126,150,155,177,187,197,199,200]. Designed and illustrated by the authors of the present work.

coatings were evenly distributed over the surface, strongly adhered and were well differentiated. The SAOS-2 proliferation studies conducted at 37 °C were also carried out in [197]. The MAO process favoured the integration of the cells as they were evenly distributed over the shell and showed a spherical morphology. Moreover, SAOS-2 cells showed a faster proliferation rate to the oxide layer formed on Ti-6Al-4V than Ti-6Al-7Nb. *In-vitro* studies with hBMSCs were performed by Sowa et al. [126], who deposited a coating on Ti-13Nb-13Zr. For the coating deposited at 400 V and in an aqueous electrolyte solution with 1 mol/dm^3 $Ca(H_2PO_2)_2$, the viability of hBMSCs after 10 days of cultivation was approximately the same. However, after 21 days of breeding, the viability dropped significantly. In addition, decreased hBMSCs ALP activity was reported compared to the uncoated sample. On the other hand, the collagen production was increased by about 25-fold and the ECM mineralization was increased by about 60-fold. For the coating, it was deposited at a voltage of 400 V and in an aqueous electrolyte solution with 0.1 mol/dm^3 $Ca(H_2PO_2)_2$ and 0.1 mol/dm^3 H_3PO_4, there was an increase in cell viability after 10 days, but also a decrease after 21 days. Under these conditions, the MAO coating did not affect the activity of ALP, collagen production and ECM mineralization of hBMSCs. In [120] other cells were used, namely MC3T3-E1 cells derived from mouse tissue. The MAO coating deposited on Ti-3Zr-2Sn-3Mo-25Nb was porous and contained an active NH_2^- group as well as Ca and P ions. Their presence strongly influenced the response of cells, which showed good proliferation and differentiation. In [155] cytocompatibility of the modified Ti-13Nb-13Zr samples was determined by the MTT cell viability assay using MG-63 osteoblast-like cells. MAO was carried out in an alkaline solution with various bioactive additives: tricalcium phosphate, wollastonite or silica at a concentration of 150 g/dm^3. The research confirmed that the presence of Ca, P and Si (from wollastonite) in the coatings stimulates cellular metabolism better than layers composed of tricalcium phosphate or silica particles. On the surface deposited in the electrolyte with the addition of tricalcium phosphate, many cells died, while on the coatings deposited in the electrolyte with the addition of wollastonite, only single dead cells were observed. Wollastonite (and thus Ca, P and Si) promote the adhesion and proliferation of cells on the oxide layers formed in the PEO process. The positive response to MG-63 cells proliferation on the coating with calcium and phosphorus ions was also confirmed in [177]. In [200], the proliferation of fHOb cells was carried out for 26 days on various media subjected to the MAO process. The nature of metabolic activity, collagen production as well as matrix formation and mineralization were comparable on β-Ti-13Nb-13Zr and β-Ti-45Nb coatings to CP α-Ti and (α+β)-Ti-6Al-4V coatings. The addition of phosphorus to the electrolyte in the MAO process increases the possibility of osseointegration without inhibiting the activity of osteoblasts or introducing an unwanted inflammatory response.

In Table 3, the selected published data of biological *in-vitro* and/or *in-vivo* properties of MAO coating on titanium and its alloys are specified.

Table 3 The selected published data of biological *in-vitro* and/or *in-vivo* properties of MAO coating on titanium and its alloys

Material	Immersion Test (Environment; Apatite Forming Ability)	*In-vitro* Assay		*In-vivo* Assay		References
		Cells	Results	Model	Results	
CP-Ti (Grade 2)	Simulated Body Fluid; yes	MG-63	Cell adhesion and proliferation noted on deposited coatings. The number of pseudopodia responsible for cell anchored depends on the process parameters.	-	-	[196]
CP-Ti (Grade 2)	Simulated Body Fluid; yes	hGFs	No effect of the coating on the viability of fibroblast cells. The coating is biocompatible as it promotes adhesion and proliferation of fibroblasts. Protein adsorption increased (almost 2-fold) compared to uncoated CP-Ti.	-	-	[150]
CP-Ti (Grade 2)	--	MC3T3-E1	Exalted biocompatibility with no explicit cytotoxicity. The elongation of duration process occasion increasing cell proliferation after incubations for 1 and 5 days, which is due to the accrued amount of HA on the coatings. Good viability of cells confirmed.	-	-	[182]
CP-Ti (Grade 4)	-	MC3T3-E1	The bioactivity of four different samples was tested: after HA blasting, after sandblasting and acid etching (SLA), after SLA and anodic oxidation (AO) as well as after SLA and MAO. Cellular attachment and proliferation are higher for SLA-AO and SLA-MAO compared to the rest. Adhesion strength was higher for SLA-AO than for SLA-MAO.	-	-	[30]
CP-Ti (Grade 4)	-	MC3T3-E1	Improved cell proliferation and differentiation have been found in some areas of the coating.			[201]
CP-Ti	-	MG-63	Cell proliferation varies depending on the solution used. The addition of calcium acetate causes a reduction in cell proliferation by about 15% compared to the coating deposited without calcium acetate. Deposition of the RGD-derivative of (3 - {[3- (2,5-dioxo-2,5-dihydro-1H-pyrrol-1-yl) propanoyl] amino} -1-hydroxypropane-1,1-diyl) -bis - (phosphonic acid) (RGDC-BMPS-β) on the coating (oxidized without calcium acetate) gives the best cell adhesion and proliferation. The bioactivity of the sample with RGD is 37% elevated compared to the coating without RGD.	-	-	[149]
CP-Ti	Simulated Body Fluid; yes	MC3T3-E1	The formation of the PEO coating in the doped-Ag bath has a positive effect on the differentiation of cells. The coating doped with Ag_2O exhibits increased cell differentiation activity compared to the coating doped with Ag.			[42]
CP-Ti Ti-6Al-4V	-	fHOb	Comparable nature of metabolic activity, collagen production, matrix formation and mineralization for each medium. No difference in the release of TNF-α and IL-10 cytokines from CD14+ monocytes. Possibility of osseointegration without inhibiting osteoblast activity or introducing an unwanted inflammatory response.	-	-	[200]
Ti-6Al-4V	Simulated Body Fluid; yes	-	-	-	-	[121]

Material	Immersion Test (Environment; Apatite Forming Ability)	*In-vitro* Assay		*In-vivo* Assay		References
		Cells	Results	Model	Results	
Ti-6Al-4V	-	MC3T3-E1 hGFs	The proliferative capacities similar for each sample in the number of adhered cells on the coating after one day. Further cultivation reveals that the number of cells augments along with increasing concentration of yttrium and was considerably higher than non-doped sample.	-	-	[152]
Ti-6Al-4V	-	MC3T3-E1	Osteoblast growth and differentiation observed for each sample. The values vary depending on the chemical composition of the electrolyte. The highest cytocompatibility was demonstrated for the pure Ti-4Al-6V alloy but the values for the coatings were at a similar level. Differentiation of preoastablasts was possible on each sample and the values were similar. The PEO-Si/F-180s response was the highest.	-	-	[202]
Ti-6Al-4V	-	SAOS-2	The rate of cell proliferation, alkaline phosphatase activity, and cell adhesion for the MAO shell increased significantly. The cell lines were evenly distributed over the surface, strongly adhered and were well differentiated.	-	-	[55]
Ti-6Al-4V	Simulated Body Fluid; yes	-	-	-	-	[153]
Ti-6Al-4V	-	MG-63	Initial cell attachment is better for a MAO-coated sample. Samples after the MAO process exhibit better cell proliferation compared to the uncoated alloy only after 7 days of cultivation. On days 1 and 3, they show lower proliferation rates than the untreated sample.	-	-	[158]
Ti-6Al-4V	-	MC3T3-E1	The proliferation ability of osteoblasts is relevantly enhanced after MAO. The hierarchical morphology with grooves/pores of coating manufactured in aqueous electrolyte with 0.1 $Na_2B_4O_7$ + 0.25 KOH displays more preferable adhesion and spreading of osteoblasts (in comparison with coating produced in aqueous electrolyte with 0.1 $Na_2B_4O_7$).	-	-	[203]
Ti-6Al-4V Ti-6Al-7Nb	Simulated Body Fluid; yes	SAOS-2	The MAO process greatly promotes cell integration. SAOS-2 cells show a faster proliferation rate to the oxide layer of Ti-6Al-4V alloy than Ti-6Al-7Nb	--	-	[197]
Ti-6Al-7Nb	Simulated Body Fluid; yes	MG-63	The cell line is well distributed on the surface of the sample produced in an aqueous electrolyte solution with 7 g/dm^3 Na_2HPO_4 + 20 g/dm^3 $C_4H_6O_4Ca{\cdot}H_2O$	-	-	[177]
Selective Laser Melted Ti-6Al-4V	Simulated Body Fluid; yes	-	-	-	-	[154]
Ti-13Nb-13Zr	Simulated Body Fluid; yes	hBMSCs	Viability negative. Collagen production depends on mineralization ECM depends on electrolyte composition.	-	-	[126]

Material	Immersion Test (Environment; Apatite Forming Ability)	*In-vitro* Assay		*In-vivo* Assay		References
		Cells	Results	Model	Results	
Ti-13Nb-13Zr	Hank's solution; yes	-	-	-	-	[33]
Ti-13Nb-13Zr	Simulated Body Fluid; questionable	hBMSCs	Cell viability better on all post-MAO samples compared to uncoated alloy. Cell adhesion, proliferation and differentiation more significant for calcium lactate electrolyte coatings than for calcium formate coatings.	-	-	[195]
Ti-13Nb-13Zr	Simulated Body Fluid; yes	MG-63	Many dead cells on the surface produced from tricalcium phosphate. On the coatings produced with wollastonite, only single dead cells and an increase in cell adhesion and proliferation.	-	-	[155]
Titanium alloy similar to β-Ti-13Nb-13Zr β-Ti45Nb	-	fHOb	Comparable nature of metabolic activity, collagen production, matrix formation and mineralization for each medium. No difference in the release of TNF-α and IL-10 cytokines from CD14+ monocytes. Possibility of osseointegration without inhibiting osteoblast activity or introducing an unwanted inflammatory response.	--	-	[200]
Ti-29Nb-13Ta-4.6Zr	Hank's solution without glucose; yes	-	-	-	-	[6]
Ti-15Zr-7.5Mo	Hank's solution without glucose; no	-	-	-	-	[9]
Ti-3Zr-2Sn-3Mo-25Nb	Simulated Body Fluid; yes	MC3T3-E1	Significant increase in cell proliferation and differentiation.	Rabbit	The activated MAO coating is covered with new bone and no fibrous tissue. On the surface of the MAO coating without activation, only slight osteoidal and lamellar deformations, not having any specific features of bone ingrowth.	[120]
Ti-15Mo	-	MG-63	The samples after the MAO process in the copper-containing bath exhibit more beneficial adhesion, growth and proliferation of cells (compared to the uncoated alloy and the alloy after the MAO process in the bath without the addition of copper). The presence of copper in the coatings has an advantageous impact on the adhesion and viability of cells.	-	-	[204]

3.5. In-vivo assays of coating in micro-arc oxidation

In-vitro tests are a valuable clue regarding the potential behaviour of the implant in the human body [109]. Unfortunately, their results cannot be directly translated into the behaviour of the implant in the human body. Therefore, after the positive results of *in-vitro* tests, it is possible to conduct *in-vivo* tests, as their results also show the dynamics of the growth of the connection between the tissue and the implant. *In-vivo* studies are essential before starting clinical trials [110,117]. Sen et al. [120] conducted *in-vivo* studies on rabbits of the coating deposited on Ti-3Zr-2Sn-3Mo-25Nb. Two types of coatings were tested: only after the MAO process and the coating activated with the aid of the ceric ion technique. The surface morphology of the implants was determined after 2, 4, 12 weeks of implantation. After 12 weeks, almost the entire surface of the active MAO coating was covered with new bone and no fibrous tissue was found at the interface. On the other hand, on the surface of the MAO coating without activation, only small osteoidal and lamellar deformations were found, which do not have features responsible for bone ingrowth. *In-vivo* studies on rabbits were carried out in [173], where Ti-13Cr-3Al-1Fe implants covered with MAO coating were placed in the distal femora. Observations were made 4, 8 or 12 weeks after the surgery. It was found that MAO-coated implants allowed better bone induction compared to the uncoated sample. The coatings were osteogenic in nature, possibly due to the alignment of the lattice with apatites and numerous hydroxyl groups. These types of implants may find application in future clinical application.

In Table 3, the selected published data of biological *in-vitro* and/or *in-vivo* proper-ties of MAO coating on titanium and its alloys are shown.

Although plasma electrolytic oxidation is a relatively modern method of producing coatings on various materials, it is currently experiencing a blooming period. Similarly to anodic oxidation, it allows the modification of the properties of coatings (morphology, thickness, chemical composition, crystallinity, roughness, mechanical and tribological properties, corrosion resistance and wettability as well surface free energy) by changing the process parameters (especially the variables are voltage, current density, temperature and composition of electrolyte, duration, frequency). Again, the change of a parameter is not linearly correlated with all properties of the coating. Inadequately selected parameters (e.g. too large pulse width and energy of a single pulse or too high temperature) may cause the coatings to crack. Nevertheless, a comprehensive analysis has shown that the coatings obtained by this method possess very good adhesion to the substrate and high corrosion resistance. In addition, when using electrolytes with calcium and phosphorus, the coating often consists of anatase and rutile, which significantly increase the biocompatibility of the coating. Moreover, bioactive elements or metal oxides can be successfully incorporated into the coating, which can also improve their properties.

4. Comparison of the electrochemical surface modification treatment for titanium and titanium alloys

There are many different methods of surface modification of titanium and its alloys for biomedical applications. The key is to select the appropriate technique to the requirements of a given environment of the potentially placed implant. The proper modification of the surface allows to adjust the properties of the implant. In general, electrochemical treatments can alter the surface morphology, transform the chemical composition and crystallinity of the coating, improve the wettability, corrosion and strength properties of the implant (Fig. 13), and increase osseointegration compared to uncoated material.

Table 4 presents the advantages and disadvantages of electrochemical technologies presented in this article.

Table 4. Comparison of the electrochemical technologies used for the generating coatings on titanium and its alloys [7,34,113,182,205–208]

Method	Advantages	Disadvantages
Anodic oxidation	- short processing time - simple apparatus - the possibility of depositing uniform coatings on substrates of complex shape - easy to adjust the composition, thickness and morphology of the coating - low cost of the process - possibility of creating coatings showing higher hardness, higher mechanical properties, enhanced corrosion resistance, and even better biocompatibility compared to uncoated material	- the possibility of creating various structures depending on the composition of the electrolyte (nanotubes, nanopores, nanocrystals), which can be unpredictable - sometimes thermal treatment is necessary to obtain coatings that improve biocompatibility (rutile and anatase)
Micro-arc oxidation	- short process time - relatively simple apparatus - PEO surface pretreatment is simpler compared to anodizing - creating highly adhesive coatings to the substrate	- the process consumes a lot of electricity and energy - due to the above most often used for samples with a small surface (less than 0.5 m^2)

Method	Advantages	Disadvantages
	- coating with high hardness, excellent abrasion resistance and increased corrosion resistance - the most common forms are anatase or anatase and rutile, which significantly improves the biocompatibility of the biomaterial	- machining of large items most often includes elements of high added value in the defence and aviation industries. - necessary control of inherent porosity, which can reach up to 20% - cooling is required while the process is running; otherwise, the electrolytic system may overheat

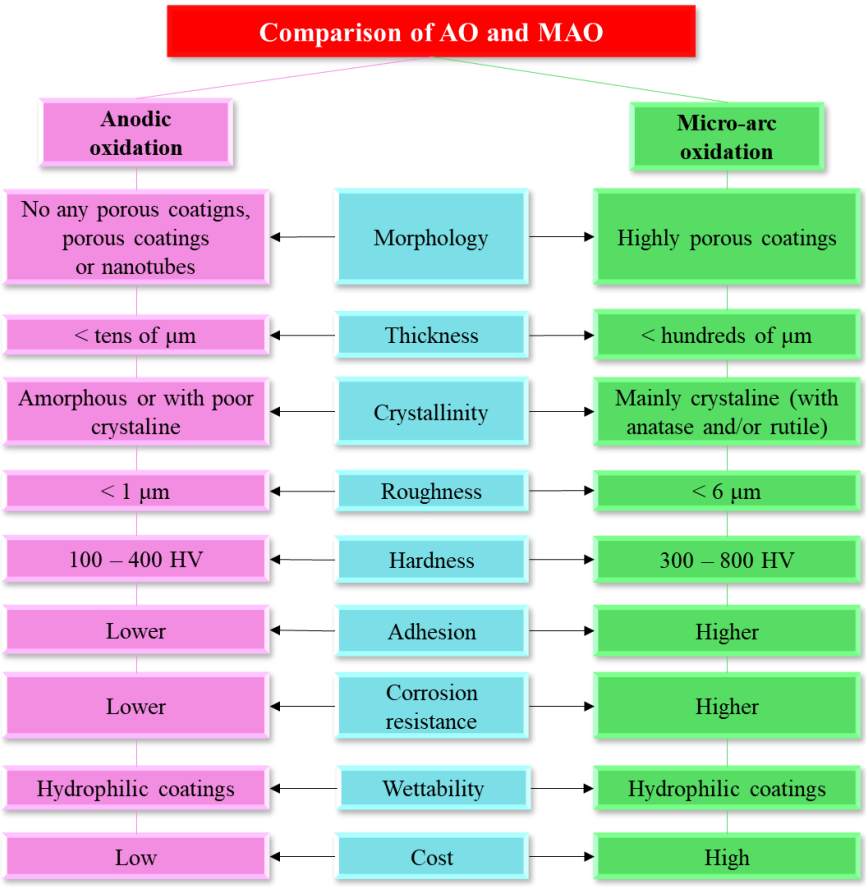

Fig. 13 Comparison of anodic oxidation and micro-arc oxidation coatings with regard to their potential use in biomedical applications. All properties of the coating depend on the parameters used during the process. Designed and illustrated by the authors of the present work.

5. Conclusions and future aspects

Although titanium and its alloys have many fascinating properties (high strength, high corrosion resistance, appropriate chemical composition - a small amount of toxic elements), the problem of their bioactivity in the body still remains. Therefore, various surface treatments (physical, chemical, biological, electrochemical) are used to reproduce the human bone. The purpose of each implant treatment is to change the morphology and chemical composition of the coating, which is to result in improving the life of the implant in the human body and minimizing the possibility of stress shielding. Nevertheless, undesirable reactions of the body may still occur. The most common complications include infections, embolism, thrombosis and loosening of the implant.

Electrochemical treatment has many significant advantages that are necessary to improve the mechanical and biological properties of the material. It is characterized by a short process duration, relatively low costs, simple apparatus, the possibility of depositing any shapes and easy modification of parameters, resulting in obtaining coatings of different quality. Often these methods use electrolytes/suspensions containing Ca, P, HA or chitosan, which support the osseointegration process and improve corrosion and wear resistance of the coatings. Furthermore, it is increasingly common to use compounds with antibacterial properties in electrolytes (most often Ag, Cu, Zn nanoparticles or their oxides), which exhibit bactericidal activity against *S. aureus* and *E. coli*.

Despite the many advantages of anodic oxidation and micro-arc oxidation as a coating technology for titanium and its alloys, there are significant disadvantages and challenges to which special attention should be paid. Future

research should rely on an in-depth understanding of the mechanisms of coating formation (including nanotubes) in electrochemical techniques and a hybrid combination of several coating deposition techniques. In addition, it might be expedient to incorporate drugs into the coatings.

The mechanical and biological properties as well as the corrosion resistance of electrochemical coatings quoted in the literature are different for the same substrate. Big differences result mainly from the process conditions: voltage, temperature, electrolyte composition and duration of the process. It is expedient to optimize these components so that the coated material meets the requirements for implants. New biocompatible coatings are immediately required; therefore, a combination of electrochemical or other methods like heat treatment or plasma surface modification could prove highly effective modification of titanium and its alloys, which would allow their efficient and wide application. The development of MAO coatings with a mixture of natural and/or synthetic polymers and nanoparticles, which are already successfully used individually in tissue engineering, should also be considered. In this search, particular attention should be paid to the corrosion resistance and surface free energies of the coatings, as there are few studies that consider these aspects. It may be particularly important to investigate the surface free energy of the coatings and its influence on the bioactivity of the implant, and to find the correlation between this feature of the coating and the parameters of the MAO process. However, the development of coatings with excellent anti-corrosion properties will enable their use not only in biomedicine, but also in marine, automobile, aerospace or military. Besides, it is crucial to study and thoroughly understand the mechanism of coating formation during the MAO process.

Author Contributions: Conceptualization, B.M.-K. and A.O.; formal analysis, B.M.-K. and A.O.; investigation, B.M.-K.; writing—original draft preparation, B.M.-K.; writing—review, A.O; writing – editing, B.M.-K.; visualization, B.M.-K. and A.O.; supervision, A.O. All authors have read and agreed to the published version of the manuscript.

Funding: This research received no external funding.

Institutional Review Board Statement: Not applicable.

Informed Consent Statement: Not applicable.

Conflicts of Interest: The authors declare no conflict of interest.

Acknowledgement: The authors would like to express our gratitude to Dr. Mohammad Reza Saeb from Department of Polymer Technology, Gdansk University of Technology, Gdansk, Poland, for substantive advice and guidance as well as ethical support that were provided during the writing of the paper.

References

[1] H. Chouirfa, H. Bouloussa, V. Migonney, C. Falentin-Daudré, Review of titanium surface modification techniques and coatings for antibacterial applications, Acta Biomater. 83 (2019) 37–54. https://doi.org/10.1016/j.actbio.2018.10.036.
[2] M. Geetha, A.K. Singh, R. Asokamani, A.K. Gogia, Ti based biomaterials, the ultimate choice for orthopaedic implants - A review, Prog Mater Sci. 54 (2009) 397–425. https://doi.org/10.1016/j.pmatsci.2008.06.004.
[3] F. H. Froes, Titanium: Physical Metallurgy, Processing, and Applications. ASM International, Materials Park (2015).
[4] X. Liu, P.K. Chu, C. Ding, Surface modification of titanium, titanium alloys, and related materials for biomedical applications, Mater Sci Eng R Rep. 47 (2004) 49–121. https://doi.org/10.1016/j.mser.2004.11.001.
[5] M. Dziaduszewska, A. Zieliński, Structural and material determinants influencing the behavior of porous Ti and its alloys made by additive manufacturing techniques for biomedical applications, Materials. 14 (2021) 1–48. https://doi.org/10.3390/ma14040712.
[6] Y. Tsutsumi, M. Niinomi, M. Nakai, H. Tsutsumi, H. Doi, N. Nomura, T. Hanawa, Micro-arc oxidation treatment to improve the hard-tissue compatibility of Ti-29Nb-13Ta-4.6Zr alloy, Appl Surf Sci. 262 (2012) 34–38. https://doi.org/10.1016/j.apsusc.2012.01.024.
[7] L.C. Zhang, L.Y. Chen, L. Wang, Surface Modification of Titanium and Titanium Alloys: Technologies, Developments, and Future Interests, Adv Eng Mater. 22 (2020). https://doi.org/10.1002/adem.201901258.
[8] P. Sahoo, S.K. Das, J. Paulo Davim, Tribology of materials for biomedical applications, in: Mechanical Behaviour of Biomaterials, Elsevier, 2019: pp. 1–45. https://doi.org/10.1016/B978-0-08-102174-3.00001-2.
[9] Y. Tsutsumi, M. Ashida, K. Nakahara, A. Serizawa, H. Doi, C.R. Grandini, L.A. Rocha, T. Hanawa, Micro arc oxidation of Ti-15Zr-7.5Mo alloy, in: Mater Trans, Japan Institute of Metals (JIM), 2016: pp. 2015–2019. https://doi.org/10.2320/matertrans.MI201513.
[10] N. Asgari, M. Rajabi, Enhancement of mechanical properties of hydroxyapatite coating prepared by electrophoretic deposition method, Int J Appl Ceram Technol. 18 (2021) 147–153. https://doi.org/10.1111/ijac.13638.
[11] H. Maleki-Ghaleh, J. Khalil-Allafi, Characterization, mechanical and *in vitro* biological behavior of hydroxyapatite-titanium-carbon nanotube composite coatings deposited on NiTi alloy by electrophoretic deposition, Surf Coat Technol. 363 (2019) 179–190. https://doi.org/10.1016/j.surfcoat.2019.02.029.
[12] I. Kovrlija, J. Locs, D. Loca, Incorporation of Barium Ions into Biomaterials: Dangerous Liaison or Potential Revolution?, Materials. 14 (2021) 5772. https://doi.org/10.3390/ma14195772.

[13] J. Alipal, N.A.S. Mohd Pu'ad, N.H.M. Nayan, N. Sahari, H.Z. Abdullah, M.I. Idris, T.C. Lee, An updated review on surface functionalisation of titanium and its alloys for implants applications, in: Mater Today Proc, Elsevier Ltd, 2019: pp. 270–282. https://doi.org/10.1016/j.matpr.2021.01.499.
[14] N.A. Costa, D.R.N. Correa, P.N. Lisboa-Filho, T.S.P. Sousa, C.R. Grandini, L.A. Rocha, Influence of the molybdenum on characteristics of oxide films produced by micro-arc oxidation on Ti-15Zr-based alloys, Surf Coat Technol. 408 (2021) 126856. https://doi.org/10.1016/j.surfcoat.2021.126856.
[15] N. Jagadeeshanayaka, S. Awasthi, S.C. Jambagi, C. Srivastava, Bioactive surface modifications through thermally sprayed hydroxyapatite composite coatings: a review of selective reinforcements, Biomater Sci. 10 (2022) 2484–2523. https://doi.org/10.1039/D2BM00039C.
[16] M. Chen, X.-Q. Wang, E.-L. Zhang, Y.-Z. Wan, J. Hu, Antibacterial ability and biocompatibility of fluorinated titanium by plasma-based surface modification, Rare Metals. 41 (2022) 689–699. https://doi.org/10.1007/s12598-021-01808-y.
[17] L. Wang, Q. Luo, X. Zhang, J. Qiu, S. Qian, X. Liu, Co-implantation of magnesium and zinc ions into titanium regulates the behaviors of human gingival fibroblasts, Bioact Mater. 6 (2021) 64–74. https://doi.org/10.1016/j.bioactmat.2020.07.012.
[18] R. Gabor, L. Cvrček, M. Doubková, V. Nehasil, J. Hlinka, P. Unucka, M. Buřil, A. Podepřelová, J. Seidlerová, L. Bačáková, Hybrid coatings for orthopaedic implants formed by physical vapour deposition and microarc oxidation, Mater Des. 219 (2022) 110811. https://doi.org/10.1016/j.matdes.2022.110811.
[19] K. Švagrová, D. Horkavcová, E. Jablonská, A. Helebrant, Titania- based sol–gel coatings with Ag , Ca- P applied on titanium substrate developed for implantation, J Biomed Mater Res B Appl Biomater. 110 (2022) 115–124. https://doi.org/10.1002/jbm.b.34895.
[20] A. Radtke, M. Grodzicka, M. Ehlert, T. Muzioł, M. Szkodo, M. Bartmański, P. Piszczek, Studies on Silver Ions Releasing Processes and Mechanical Properties of Surface-Modified Titanium Alloy Implants, Int J Mol Sci. 19 (2018) 3962. https://doi.org/10.3390/ijms19123962.
[21] B. Ribeiro, R. Offoiach, E. Rahimi, E. Salatin, M. Lekka, L. Fedrizzi, On growth and morphology of TiO_2 nanotubes on ti6al4v by anodic oxidation in ethylene glycol electrolyte: Influence of microstructure and anodization parameters, Materials. 14 (2021). https://doi.org/10.3390/ma14102540.
[22] M. Michalska-Domańska, M. Łazińska, J. Łukasiewicz, J.M.C. Mol, T. Durejko, Self-organized anodic oxides on titanium alloys prepared from glycol-and glycerol-based electrolytes, Materials. 13 (2020) 1–12. https://doi.org/10.3390/ma13214743.
[23] M.R. Kaluđerović, J.P. Schreckenbach, H.-L. Graf, Titanium dental implant surfaces obtained by anodic spark deposition – From the past to the future, Mater Sci Eng C. 69 (2016). https://doi.org/10.1016/j.msec.2016.07.068.
[24] S. Rafieinasab, J. Sedaghatnia, Electrocoating of Titanium Nanoparticle and Investigation of its Characters, Medbiotech J. 4 (2020) 19–021. https://doi.org/10.22034/mbt.2020.105878.
[25] I.P. Torres-Avila, I.I. Padilla-Martínez, N. Pérez-Hernández, A.E. Bañuelos-Hernández, J.C. Velázquez, J.L. Castrejón-Flores, E. Hernández-Sánchez, Surface modification of the Ti-6Al-4V alloy by anodic oxidation and its effect on osteoarticular cell proliferation, Coatings. 10 (2020). https://doi.org/10.3390/COATINGS10050491.
[26] M. Bartmanski, B. Cieslik, J. Glodowska, P. Kalka, L. Pawlowski, M. Pieper, A. Zielinski, Electrophoretic deposition (EPD) of nanohydroxyapatite - nanosilver coatings on Ti13Zr13Nb alloy, Ceram Int. 43 (2017) 11820–11829. https://doi.org/10.1016/j.ceramint.2017.06.026.
[27] S.R. Fardi, H. khorsand, R. Askarnia, R. Pardehkhorram, E. Adabifiroozjaei, Improvement of biomedical functionality of titanium by ultrasound-assisted electrophoretic deposition of hydroxyapatite-graphene oxide nanocomposites, Ceram Int. 46 (2020) 18297–18307. https://doi.org/10.1016/j.ceramint.2020.05.049.
[28] J.P.A. Carobolante, K.B. da Silva, J.A.M. Chaves, M.F. Dias Netipanyj, K.C. Popat, A.P.R. Alves Claro, Nanoporous layer formation on the Ti10Mo8Nb alloy surface using anodic oxidation, Surf Coat Technol. 386 (2020). https://doi.org/10.1016/j.surfcoat.2020.125467.
[29] K. Zhurakivska, N. Ciacci, G. Troiano, V.C.A. Caponio, R. Scrascia, L. Pallecchi, L. lo Muzio, F. Arena, Nitride-Coated and Anodic-Oxidized Titanium Promote a Higher Fibroblast and Reduced Streptococcus gordonii Proliferation Compared to the Uncoated Titanium, Prosthesis. 2 (2020) 333–339. https://doi.org/10.3390/prosthesis2040031.
[30] J. Kim, H. Lee, T.S. Jang, D. Kim, C.B. Yoon, G. Han, H.E. Kim, H. do Jung, Characterization of titanium surface modification strategies for osseointegration enhancement, Metals (Basel). 11 (2021). https://doi.org/10.3390/met11040618.
[31] Ö. Bayrak, H. Ghahramanzadeh Asl, A. Ak, Protein adsorption, cell viability and corrosion properties of Ti6Al4V alloy treated by plasma oxidation and anodic oxidation, International Journal of Minerals, Metallurgy and Materials. 27 (2020) 1269–1280. https://doi.org/10.1007/s12613-020-2020-5.
[32] M. Bartmanski, A. Zielinski, M. Jazdzewska, J. Głodowska, P. Kalka, Effects of electrophoretic deposition times and nanotubular oxide surfaces on properties of the nanohydroxyapatite/nanocopper coating on the Ti13Zr13Nb alloy, Ceram Int. 45 (2019) 20002–20010. https://doi.org/10.1016/j.ceramint.2019.06.258.
[33] M. Dziaduszewska, M. Shimabukuro, T. Seramak, A. Zielinski, T. Hanawa, Effects of micro-arc oxidation process parameters on characteristics of calcium-phosphate containing oxide layers on the selective laser melted Ti13Zr13Nb alloy, Coatings. 10 (2020). https://doi.org/10.3390/COATINGS10080745.
[34] K.-H. Kim, N. Ramaswamy, Electrochemical surface modification of titanium in dentistry, Dent Mater J. 28 (2009) 20-36. https://doi.org/ 10.4012/dmj.28.20.
[35] M. Kaur, K. Singh, Review on titanium and titanium based alloys as biomaterials for orthopaedic applications, Mater Sci Eng C. 102 (2019) 844–862. https://doi.org/10.1016/j.msec.2019.04.064.
[36] M. Geetha, A.K. Singh, R. Asokamani, A.K. Gogia, Ti based biomaterials, the ultimate choice for orthopaedic implants - A review, Prog Mater Sci. 54 (2009) 397–425. https://doi.org/10.1016/j.pmatsci.2008.06.004.
[37] A. Kumar, M.K. Kushwaha, Surface modification of titanium alloy by anodic oxidation method to improve its biocompatibility, Curr Sci. 120 (2021) 907-914.

[38] B. Wu, S. Xiong, Y. Guo, Y. Chen, P. Huang, B. Yang, Tooth-colored bioactive titanium alloy prepared with anodic oxidation method for dental implant application, Mater Lett. 248 (2019) 134–137. https://doi.org/10.1016/j.matlet.2019.04.015.
[39] B.L. Pereira, G. Beilner, C.M. Lepienski, G.B. de Souza, N.K. Kuromoto, E.S. Szameitat, A.N.S. Peng, J.Y. Lee, A.P.R.A. Claro, M.J.D. Nugent, Scratch-resistant and well-adhered nanotube arrays produced via anodizing process on β-titanium alloy, Mater Today Commun. 26 (2021). https://doi.org/10.1016/j.mtcomm.2020.101947.
[40] G. Louarn, L. Salou, A. Hoornaert, P. Layrolle, Nanostructured surface coatings for titanium alloy implants, J Mater Res. 34 (2019) 1892–1899. https://doi.org/10.1557/jmr.2019.39.
[41] A. Sobolev, A. Kossenko, K. Borodianskiy, Study of the effect of current pulse frequency on Ti-6Al-4V alloy coating formation by micro arc oxidation, Materials. 12 (2019). https://doi.org/10.3390/ma12233983.
[42] X. Zhang, Y. Lv, G. Cai, S. Fu, L. Yang, Y. Ma, Z. Dong, Reactive incorporation of Ag into porous TiO_2 coating and its influence on its microstructure, *in vitro* antibacterial efficacy and cytocompatibility, Prog Nat Sci: Mater Int. 31 (2021) 215–229. https://doi.org/10.1016/j.pnsc.2021.02.002.
[43] M.B. Sedelnikova, E.G. Komarova, Y.P. Sharkeev, A. v. Ugodchikova, T. v. Tolkacheva, J. v. Rau, E.E. Buyko, V. v. Ivanov, V. v. Sheikin, Modification of titanium surface via Ag-, Sr- and Si-containing micro-arc calcium phosphate coating, Bioact Mater. 4 (2019) 224–235. https://doi.org/10.1016/j.bioactmat.2019.07.001.
[44] M. Jarosz, J. Grudzień, J. Kapusta-Kołodziej, A. Chudecka, M. Sołtys, G.D. Sulka, Anodization of titanium alloys for biomedical applications, in: Nanostructured Anodic Metal Oxides, Elsevier, 2020: pp. 211–275. https://doi.org/10.1016/b978-0-12-816706-9.00007-8.
[45] R. Hang, F. Zhao, X. Yao, B. Tang, P.K. Chu, Self-assembled anodization of NiTi alloys for biomedical applications, Appl Surf Sci. 517 (2020). https://doi.org/10.1016/j.apsusc.2020.146118.
[46] J. Lausmaa, Mechanical, Thermal, Chemical and Electrochemical Surface Treatment of Titanium, in: Titanium in Medicine, 1st ed., SpringerLink, (2001), pp. 21-266. https://doi.org/10.1007/978-3-642-56486-4_8.
[47] B. Yang, Preparation of bioactive titanium metal via anodic oxidation treatment, Biomaterials. 25 (2004) 1003-1010. https://doi.org/10.1016/S0142-9612(03)00626-4.
[48] D.R.N. Correa, L.A. Rocha, A.R. Ribeiro, S. Gemini-Piperni, B.S. Archanjo, C.A. Achete, J. Werckmann, C.R.M. Afonso, M. Shimabukuro, H. Doi, Y. Tsutsumi, T. Hanawa, Growth mechanisms of Ca- and P-rich MAO films in Ti-15Zr-xMo alloys for osseointegrative implants, Surf Coat Technol. 344 (2018) 373–382. https://doi.org/10.1016/j.surfcoat.2018.02.099.
[49] L. Liu, L. Wu, X. Chen, D. Sun, Y. Chen, G. Zhang, X. Ding, F. Pan, Enhanced protective coatings on Ti-10V-2Fe-3Al alloy through anodizing and post-sealing with layered double hydroxides, J Mater Sci Technol. 37 (2020) 104–113. https://doi.org/10.1016/j.jmst.2019.07.032.
[50] G. Marenzi, G. Spagnuolo, J.C. Sammartino, R. Gasparro, A. Rebaudi, M. Salerno, Micro-scale surface patterning of titanium dental implants by anodization in the presence of modifying salts, Materials. 12 (2019). https://doi.org/10.3390/ma12111753.
[51] X. Zhang, Y. Wan, Z. Liu, H. Wang, M. Yu, A. Liu, D. Zhang, Preparation and bioactive response of super-hydrophilic surface on selective laser melting titanium, in: Procedia CIRP, Elsevier B.V., 2020: pp. 222–227. https://doi.org/10.1016/j.procir.2020.05.145.
[52] Y. Li, Y. You, B. Li, Y. Song, A. Ma, B. Chen, W. Han, C. Li, Improved Cell Adhesion and Osseointegration on Anodic Oxidation Modified Titanium Implant Surface, J Hard Tissue Biol. 28 (2019) 13–20.
[53] L. Mohan, C. Dennis, N. Padmapriya, C. Anandan, N. Rajendran, Effect of Electrolyte Temperature and Anodization Time on Formation of TiO_2 Nanotubes for Biomedical Applications, Mater Today Commun. 23 (2020). https://doi.org/10.1016/j.mtcomm.2020.101103.
[54] A. Nemtsov, P. Kirshkov, Electrochemical Characterization of Titanium Oxide Nanoparticle through Anodic Oxidation, Medbiotech J. 4 (2020) 83–86. https://doi.org/10.22034/MBT.2020.109583.
[55] Y.W. Lim, S.Y. Kwon, D.H. Sun, H.E. Kim, Y.S. Kim, Enhanced cell integration to titanium alloy by surface treatment with microarc oxidation: A pilot study, in: Clin Orthop Relat Res, Springer New York, 2009: pp. 2251–2258. https://doi.org/10.1007/s11999-009-0879-6.
[56] X. Lu, S. Xiong, Y. Chen, F. Zhao, Y. Hu, Y. Guo, B. Wu, P. Huang, B. Yang, Effects of statherin on the biological properties of titanium metals subjected to different surface modification, Colloids Surf B Biointerfaces. 188 (2020). https://doi.org/10.1016/j.colsurfb.2020.110783.
[57] S. Durdu, G. Cihan, E. Yalcin, A. Altinkok, Characterization and mechanical properties of TiO_2 nanotubes formed on titanium by anodic oxidation, Ceram Int. 47 (2021) 10972–10979. https://doi.org/10.1016/j.ceramint.2020.12.218.
[58] V. Zwilling, M. Aucouturier, E. Darque-Ceretti, Anodic oxidation of titanium and TA6V alloy in chromic media. An electrochemical approach, Electrochim Acta. 45 (1999). https://doi.org/10.1016/S0013-4686(99)00283-2.
[59] V.T. Nguyen, T.C. Cheng, T.H. Fang, M.H. Li, The fabrication and characteristics of hydroxyapatite film grown on titanium alloy Ti-6Al-4V by anodic treatment, Journal of Materials Research and Technology. 9 (2020) 4817–4825. https://doi.org/10.1016/j.jmrt.2020.03.002.
[60] X. Zhan, S. Li, Y. Cui, A. Tao, C. Wang, H. Li, L. Zhang, H. Yu, J. Jiang, C. Li, Comparison of the osteoblastic activity of low elastic modulus Ti-24Nb-4Zr-8Sn alloy and pure titanium modified by physical and chemical methods, Mater Sci Eng C. 113 (2020) 111018. https://doi.org/10.1016/j.msec.2020.111018.
[61] D. Shan, B. Tao, C. Fang, H. Shao, L. Xie, J. Feng, G. Yan, Anodization of titanium in reduced graphene oxide-citric acid electrolyte, Results Phys. 24 (2021). https://doi.org/10.1016/j.rinp.2021.104060.
[62] M. Mallaiah, R.K. Gupta, Surface Engineering of Titanium Using Anodization and Plasma Treatment, in: IOP Conf Ser Mater Sci Eng, IOP Publishing Ltd, 2020. https://doi.org/10.1088/1757-899X/943/1/012016.
[63] G.R.M. Matos, Surface Roughness of Dental Implant and Osseointegration, J Maxillofac Oral Surg. 20 (2021). https://doi.org/10.1007/s12663-020-01437-5.

[64] I. Gurappa, Development of appropriate thickness ceramic coatings on 316 L stainless steel for biomedical applications, Surf Coat Technol. 161 (2002) 70–78. https://doi.org/10.1016/S0257-8972(02)00380-8.
[65] L. Wu, C. Wen, G. Zhang, J. Liu, K. Ma, Influence of anodizing time on morphology, structure and tribological properties of composite anodic films on titanium alloy, Vacuum. 140 (2017) 176–184. https://doi.org/10.1016/j.vacuum.2016.12.047.
[66] M. Benčina, A. Iglič, M. Mozetič, I. Junkar, Crystallized TiO_2 Nanosurfaces in Biomedical Applications, Nanomaterials. 10 (2020). https://doi.org/10.3390/nano10061121.
[67] A. Ossowska, J.-M. Olive, A. Zieliński, A. Wojtowicz, Effect of double thermal and electrochemical oxidation on titanium alloys for medical applications, Appl Surf Sci. 563 (2021) 150340. https://doi.org/10.1016/j.apsusc.2021.150340.
[68] Y. Yokoi, Osteoblast-like Cell Proliferation, ALP Activity and Photocatalytic Activity on Sintered Anatase and Rutile Titanium Dioxide, Materials. 14 (2021). https://doi.org/10.3390/ma14164414.
[69] B. Li, L. Zhang, Y. Li, H. Li, L. Zhou, C. Liang, H. Wang, Corrosion Resistance and Biological Properties of Anatase and Rutile Coatings on a Titanium Surface, Chem Lett. 48 (2019) 1355–1357. https://doi.org/10.1246/cl.190549.
[70] Y. Han, D. Chen, J. Sun, Y. Zhang, K. Xu, UV-enhanced bioactivity and cell response of micro-arc oxidized titania coatings, Acta Biomater. 4 (2008) 1518–1529. https://doi.org/10.1016/j.actbio.2008.03.005.
[71] T. Li, K. Gulati, N. Wang, Z. Zhang, S. Ivanovski, Understanding and augmenting the stability of therapeutic nanotubes on anodized titanium implants, Mater Sci Eng C. 88 (2018) 182-195. https://doi.org/10.1016/j.msec.2018.03.007.
[72] L.E. Oi, M.-Y. Choo, H.V. Lee, H.C. Ong, S.B.A. Hamid, J.C. Juan, Recent advances of titanium dioxide (TiO_2) for green organic synthesis, RSC Adv. 6 (2016) 108741–108754. https://doi.org/10.1039/C6RA22894A.
[73] K. Wang, Y. Zhuo, J. Chen, D. Gao, Y. Ren, C. Wang, Z. Qi, Crystalline phase regulation of anatase–rutile TiO_2 for the enhancement of photocatalytic activity, RSC Adv. 10 (2020) 43592–43598. https://doi.org/10.1039/D0RA09421H.
[74] Z. Qu, X. Rausch-Fan, M. Wieland, M. Matejka, A. Schedle, The initial attachment and subsequent behavior regulation of osteoblasts by dental implant surface modification, J Biomed Mater Res A. 82A (2007) 658-668. https://doi.org/10.1002/jbm.a.31023.
[75] Y. Zhang, X. Cheng, J.A. Jansen, F. Yang, J.J.J.P. van den Beucken, Titanium surfaces characteristics modulate macrophage polarization, Mater Sci Eng C. 95 (2019) 143–151. https://doi.org/10.1016/j.msec.2018.10.065.
[76] A. Kurup, P. Dhatrak, N. Khasnis, Surface modification techniques of titanium and titanium alloys for biomedical dental applications: A review, Mater Today Proc. 39 (2021) 84-90. https://doi.org/10.1016/j.matpr.2020.06.163.
[77] M. Saini, Implant biomaterials: A comprehensive review, World J Clin Cases. 3 (2015) 52-57. https://doi.org/10.12998/wjcc.v3.i1.52.
[78] E.F. Morgan, G.U. Unnikrisnan, A.I. Hussein, Bone Mechanical Properties in Healthy and Diseased States, Annu Rev Biomed Eng. 20 (2018) 119-143. https://doi.org/10.1146/annurev-bioeng-062117-121139.
[79] W. Wu, Y. Zhu, W. Chen, S. Li, B. Yin, J. Wang, X. Zhang, G. Liu, Z. Hu, Y. Zhang, Bone Hardness of Different Anatomical Regions of Human Radius and its Impact on the Pullout Strength of Screws, Orthop Surg. 11 (2019) 270-276. https://doi.org/10.1111/os.12436.
[80] P.B.F. Soares, S.A. Nunes, S.D. Franco, R.R. Pires, D. Zanetta-Barbosa, C.J. Soares, Measurement of Elastic Modulus and Vickers Hardness of Surround Bone Implant Using Dynamic Microindentation - Parameters Definition, Braz Dent J. 25 (2014) 385-390. https://doi.org/10.1590/0103-6440201300169.
[81] J. Black, H. Sherk, J. Bonini, W.R. Rostoker, F. Schajowicz, J.O. Galante, Metallosis associated with a stable titanium-alloy femoral component in total hip replacement. A case report., J Bone Joint Surg Am. 72 (1990) 126–30.
[82] S.L. de Assis, S. Wolynec, I. Costa, Corrosion characterization of titanium alloys by electrochemical techniques, Electrochim Acta. 51 (2006) 1815-1819. https://doi.org/10.1016/j.electacta.2005.02.121.
[83] J. Lu, Enhanced Corrosion Resistance of TA2 Titanium via Anodic Oxidation in Mixed Acid System, Int J Electrochem Sci. (2017) 2763-2776. https://doi.org/10.20964/2017.04.69.
[84] J. Quinn, R. McFadden, C.-W. Chan, L. Carson, Titanium for Orthopedic Applications: An Overview of Surface Modification to Improve Biocompatibility and Prevent Bacterial Biofilm Formation, IScience. 23 (2020) 101745. https://doi.org/10.1016/j.isci.2020.101745.
[85] C. Berne, C.K. Ellison, A. Ducret, Y. v. Brun, Bacterial adhesion at the single-cell level, Nat Rev Microbiol. 16 (2018) 616–627. https://doi.org/10.1038/s41579-018-0057-5.
[86] H.-J. Wang, Y.-Y. Hsiao, Y.-P. Chen, T.-Y. Ma, C.-P. Tseng, Polarity Alteration of a Calcium Site Induces a Hydrophobic Interaction Network and Enhances Cel9A Endoglucanase Thermostability, Appl Environ Microbiol. 82 (2016) 1662–1674. https://doi.org/10.1128/AEM.03326-15.
[87] J. Katić, A. Šarić, I. Despotović, N. Matijaković, M. Petković, Ž. Petrović, Bioactive Coating on Titanium Dental Implants for Improved Anticorrosion Protection: A Combined Experimental and Theoretical Study, Coatings. 9 (2019) 612. https://doi.org/10.3390/coatings9100612.
[88] K. Das, S. Bose, A. Bandyopadhyay, Surface modifications and cell–materials interactions with anodized Ti, Acta Biomater. 3 (2007) 573–585. https://doi.org/10.1016/j.actbio.2006.12.003.
[89] A. Ossowska, Production, structure and properties of oxide layers obtained on titanium alloys used in biomedical applications, Gdańsk University of Technology Publishing, Gdańsk, 2017.
[90] J. K. Hirvonen (ed.), Ion Implantation, in: Treatise on Materials Science and Technology, Academic Press, New York, 1980.
[91] A. Liber-Kneć, S. Łagan, Surface Testing of Dental Biomaterials—Determination of Contact Angle and Surface Free Energy, Materials. 14 (2021) 2716. https://doi.org/10.3390/ma14112716.
[92] E.M. Harnett, J. Alderman, T. Wood, The surface energy of various biomaterials coated with adhesion molecules used in cell culture, Colloids Surf B Biointerfaces. 55 (2007) 90–97. https://doi.org/10.1016/j.colsurfb.2006.11.021.
[93] F. Hejda, P. Solar, J. Kousal, Surface free energy determination by contact angle measurements – a comparison of various approaches, WDS'10 Proceedings of Contributed Papers. 3 (2010) 25–30.

[94] M. Palencia, Surface free energy of solids by contact angle measurements., J Sci Technol Appl. 2 (2017) 84–93. https://doi.org/10.34294/j.jsta.17.2.17.
[95] M.M. Gentleman, E. Gentleman, The role of surface free energy in osteoblast–biomaterial interactions, Int. Mater. Rev. 59 (2014) 417–429. https://doi.org/10.1179/1743280414Y.0000000038.
[96] C. Pérez-Jorge, A. Conde, M.A. Arenas, R. Pérez-Tanoira, E. Matykina, J.J. de Damborenea, E. Gómez-Barrena, J. Esteban, *In vitro* assessment of Staphylococcus epidermidis and Staphylococcus aureus adhesion on TiO_2 nanotubes on Ti-6Al-4V alloy, J Biomed Mater Res A. 100A (2012) 1696–1705. https://doi.org/10.1002/jbm.a.34118.
[97] V.C. Mendes, R. Moineddin, J.E. Davies, The effect of discrete calcium phosphate nanocrystals on bone-bonding to titanium surfaces, Biomaterials. 28 (2007) 4748–4755. https://doi.org/10.1016/j.biomaterials.2007.07.020.
[98] M.A. Arenas, C. Pérez-Jorge, A. Conde, E. Matykina, J.M. Hernández-López, R. Pérez-Tanoira, J.J. de Damborenea, E. Gómez-Barrena, J. Esteba, Doped TiO_2 anodic layers of enhanced antibacterial properties, Colloids Surf B Biointerfaces. 105 (2013) 106–112. https://doi.org/10.1016/j.colsurfb.2012.12.051.
[99] B. Li, J. Li, C. Liang, H. Li, L. Guo, S. Liu, H. Wang, Surface Roughness and Hydrophilicity of Titanium after Anodic Oxidation, Rare Metal Materials and Engineering. 45 (2016) 858–862. https://doi.org/10.1016/S1875-5372(16)30088-1.
[100] S. Sista, C. Wen, P.D. Hodgson, G. Pande, The influence of surface energy of titanium-zirconium alloy on osteoblast cell functions *in vitro*, J Biomed Mater Res A. 97A (2011) 27–36. https://doi.org/10.1002/jbm.a.33013.
[101] E. Velasco-Ortega, A. Jos, A.M. Cameán, J. Pato-Mourelo, J.J. Segura-Egea, *In vitro* evaluation of cytotoxicity and genotoxicity of a commercial titanium alloy for dental implantology, Mutation Research/Genetic Toxicology and Environmental Mutagenesis. 702 (2010) 17-23. https://doi.org/10.1016/j.mrgentox.2010.06.013.
[102] K. Anselme, P. Davidson, A.M. Popa, M. Giazzon, M. Liley, L. Ploux, The interaction of cells and bacteria with surfaces structured at the nanometre scale, Acta Biomater. 6 (2010) 3824–3846. https://doi.org/10.1016/j.actbio.2010.04.001.
[103] L. Zhao, S. Mei, P.K. Chu, Y. Zhang, Z. Wu, The influence of hierarchical hybrid micro/nano-textured titanium surface with titania nanotubes on osteoblast functions, Biomaterials. 31 (2010) 5072–5082. https://doi.org/10.1016/j.biomaterials.2010.03.014.
[104] Y. Ammar, D. Swailes, B. Bridgens, J. Chen, Influence of surface roughness on the initial formation of biofilm, Surf Coat Technol. 284 (2015) 410–416. https://doi.org/10.1016/j.surfcoat.2015.07.062.
[105] M. Lorenzetti, I. Dogša, T. Stošicki, D. Stopar, M. Kalin, S. Kobe, S. Novak, The Influence of Surface Modification on Bacterial Adhesion to Titanium-Based Substrates, ACS Appl Mater Interfaces. 7 (2015) 1644–1651. https://doi.org/10.1021/am507148n.
[106] I. Yoda, H. Koseki, M. Tomita, T. Shida, H. Horiuchi, H. Sakoda, M. Osaki, Effect of surface roughness of biomaterials on *Staphylococcus epidermidis* adhesion, BMC Microbiol. 14 (2014) 234. https://doi.org/10.1186/s12866-014-0234-2.
[107] Y. Cao, B. Su, S. Chinnaraj, S. Jana, L. Bowen, S. Charlton, P. Duan, N.S. Jakubovics, J. Chen, Nanostructured titanium surfaces exhibit recalcitrance towards Staphylococcus epidermidis biofilm formation, Sci Rep. 8 (2018) 1071. https://doi.org/10.1038/s41598-018-19484-x.
[108] A. Ossowska, A. Zieliński, J.-M. Olive, A. Wojtowicz, P. Szweda, Influence of Two-Stage Anodization on Properties of the Oxide Coatings on the Ti-13Nb-13Zr Alloy, Coatings. 10 (2020) 707. https://doi.org/10.3390/coatings10080707.
[109] M. Gahlert, S. Roehling, C.M. Sprecher, H. Kniha, S. Milz, K. Bormann, *In vivo* performance of zirconia and titanium implants: a histomorphometric study in mini pig maxillae, Clin Oral Implants Res. 23 (2012) 281-286. https://doi.org/10.1111/j.1600-0501.2011.02157.x.
[110] L. Zhao, Y. Dang, L. Zhang, W. Song, B. Chang, T. Han, Y. Zhang, *In vivo* osseointegration of Ti implants with a strontium-containing nanotubular coating, Int J Nanomedicine. 11 (2016) 1003-1011. https://doi.org/10.2147/IJN.S102552.
[111] S. Ferraris, A. Vitale, E. Bertone, S. Guastella, C. Cassinelli, J. Pan, S. Spriano, Multifunctional commercially pure titanium for the improvement of bone integration: Multiscale topography, wettability, corrosion resistance and biological functionalization, Mater Sci Eng C. 60 (2016) 384–393. https://doi.org/10.1016/j.msec.2015.11.049.
[112] F. Simchen, M. Sieber, A. Kopp, T. Lampke, Introduction to Plasma Electrolytic Oxidation—An Overview of the Process and Applications, Coatings. 10 (2020) 628. https://doi.org/10.3390/coatings10070628.
[113] M.B. Sedelnikova, E.G. Komarova, Y.P. Sharkeev, A. v. Ugodchikova, L.S. Mushtovatova, M.R. Karpova, V. v. Sheikin, L.S. Litvinova, I.A. Khlusov, Zn-, Cu- or Ag-incorporated micro-arc coatings on titanium alloys: Properties and behavior in synthetic biological media, Surf Coat Technol. 369 (2019) 52–68. https://doi.org/10.1016/j.surfcoat.2019.04.021.
[114] M. Fazel, H.R. Salimijazi, M. Shamanian, Improvement of Corrosion and Tribocorrosion Behavior of Pure Titanium by Subzero Anodic Spark Oxidation, ACS Appl Mater Interfaces. 10 (2018) 15281–15287. https://doi.org/10.1021/acsami.8b02331.
[115] K. Nan, Y. Wang, X. Chen, C. Ning, lingyu Wang, N. Zhao, Application research of plasma-enhanced electrochemical surface ceramic-coating technology on titanium implants, J Biomed Mater Res B Appl Biomater. 75B (2005) 328–333. https://doi.org/10.1002/jbm.b.30310.
[116] A. Afshar, M.R. Vaezi, Evaluation of electrical breakdown of anodic films on titanium in phosphate-base solutions, Surf Coat Technol. 186 (2004) 398–404. https://doi.org/10.1016/j.surfcoat.2004.01.003.
[117] Y. Wang, H. Yu, C. Chen, Z. Zhao, Review of the biocompatibility of micro-arc oxidation coated titanium alloys, Mater Des. 85 (2015) 640–652. https://doi.org/10.1016/j.matdes.2015.07.086.
[118] Y. Wang, D. Lu, G. Wu, K. Chen, H. Wu, Q. Zhang, J. Yao, Effect of laser surface remelting pretreatment with different energy density on MAO bioceramic coating, Surf Coat Technol. 393 (2020) 125815. https://doi.org/10.1016/j.surfcoat.2020.125815.
[119] K. Rokosz, T. Hryniewicz, Characteristics of porous biocompatible coatings obtained on Niobium and Titanium-Niobium-Zirconium (TNZ) alloy by Plasma Electrolytic Oxidation, Mechanik. 12 (2015) 978/15-978/18. https://doi.org/10.17814/mechanik.2015.12.530.

[120] S. Yu, Z.T. Yu, G. Wang, J.Y. Han, X.Q. Ma, M.S. Dargusch, Preparation and osteoinduction of active micro-arc oxidation films on Ti-3Zr-2Sn-3Mo-25Nb alloy, Transactions of Nonferrous Metals Society of China (English Edition). 21 (2011) 573–580. https://doi.org/10.1016/S1003-6326(11)60753-X.
[121] Y.M. Wang, J.W. Guo, J.P. Zhuang, Y.B. Jing, Z.K. Shao, M.S. Jin, J. Zhang, D.Q. Wei, Y. Zhou, Development and characterization of MAO bioactive ceramic coating grown on micro-patterned Ti6Al4V alloy surface, Appl Surf Sci. 299 (2014) 58–65. https://doi.org/10.1016/j.apsusc.2014.01.185.
[122] Y. Wang, B. Jiang, T. Lei, L. Guo, Dependence of growth features of microarc oxidation coatings of titanium alloy on control modes of alternate pulse, Mater Lett. 58 (2004) 1907–1911. https://doi.org/10.1016/j.matlet.2003.11.026.
[123] L. Lara Rodriguez, P.A. Sundaram, Corrosion behavior of plasma electrolytically oxidized gamma titanium aluminide alloy in simulated body fluid, Mater Chem Phys. 181 (2016) 67–77. https://doi.org/10.1016/j.matchemphys.2016.06.034.
[124] Z. Shahri, S.R. Allahkaram, R. Soltani, H. Jafari, Optimization of plasma electrolyte oxidation process parameters for corrosion resistance of Mg alloy, J Magnes. 8 (2020) 431–440. https://doi.org/10.1016/j.jma.2018.10.001.
[125] S. Durdu, Ö.F. Deniz, I. Kutbay, M. Usta, Characterization and formation of hydroxyapatite on Ti6Al4V coated by plasma electrolytic oxidation, J Alloys Compd. 551 (2013) 422–429. https://doi.org/10.1016/j.jallcom.2012.11.024.
[126] M. Sowa, M. Piotrowska, M. Widziołek, G. Dercz, G. Tylko, T. Gorewoda, A.M. Osyczka, W. Simka, Bioactivity of coatings formed on Ti-13Nb-13Zr alloy using plasma electrolytic oxidation, Mater Sci Eng C. 49 (2015) 159–173. https://doi.org/10.1016/j.msec.2014.12.073.
[127] K. Rokosz, T. Hryniewicz, S. Gaiaschi, P. Chapon, S. Raaen, K. Pietrzak, W. Malorny, J. Salvador Fernandes, Characterization of Porous Phosphate Coatings Enriched with Magnesium or Zinc on CP Titanium Grade 2 under DC Plasma Electrolytic Oxidation, Metals (Basel). 8 (2018) 112. https://doi.org/10.3390/met8020112.
[128] T. Hryniewicz, R. Rokicki, K. Rokosz, Magnetoelectropolishing for metal surface modification, Transactions of the IMF. 85 (2007) 325–332. https://doi.org/10.1179/174591907X246537.
[129] T. Hryniewicz, K. Rokosz, J. Valíček, R. Rokicki, Effect of magnetoelectropolishing on nanohardness and Young's modulus of titanium biomaterial, Mater Lett. 83 (2012) 69–72. https://doi.org/10.1016/j.matlet.2012.06.010.
[130] N. Lin, D. Li, J. Zou, R. Xie, Z. Wang, B. Tang, Surface Texture-Based Surface Treatments on Ti6Al4V Titanium Alloys for Tribological and Biological Applications: A Mini Review, Materials. 11 (2018) 487. https://doi.org/10.3390/ma11040487.
[131] H.-Y. Wang, R.-F. Zhu, Y.-P. Lu, G.-Y. Xiao, X.-N. Ma, Y. Li, Structures and properties of layered bioceramic coatings on pure titanium using a hybrid technique of sandblasting and micro-arc oxidation, Appl Surf Sci. 282 (2013) 271–280. https://doi.org/10.1016/j.apsusc.2013.05.119.
[132] W.F. Cui, L. Jin, L. Zhou, Surface characteristics and electrochemical corrosion behavior of a pre-anodized microarc oxidation coating on titanium alloy, Mater Sci Eng C. 33 (2013) 3775–3779. https://doi.org/10.1016/j.msec.2013.05.011.
[133] L. Li, E. Yang, Z. Yan, X. Xie, W. Wei, W. Li, Effect of Pre-Anodized Film on Micro-Arc Oxidation Process of 6063 Aluminum Alloy, Materials. 15 (2022) 5221. https://doi.org/10.3390/ma15155221.
[134] F. Liu, F. Wang, T. Shimizu, K. Igarashi, L. Zhao, Formation of hydroxyapatite on Ti-6Al-4V alloy by microarc oxidation and hydrothermal treatment, Surf Coat Technol. 199 (2005) 220–224. https://doi.org/10.1016/j.surfcoat.2004.10.146.
[135] L.T. Duarte, C. Bolfarini, S.R. Biaggio, R.C. Rocha-Filho, P.A.P. Nascente, Growth of aluminum-free porous oxide layers on titanium and its alloys Ti-6Al-4V and Ti-6Al-7Nb by micro-arc oxidation, Mater Sci Eng C. 41 (2014) 343–348. https://doi.org/10.1016/j.msec.2014.04.068.
[136] C. Wang, F. Ma, P. Liu, J. Chen, X. Liu, K. Zhang, W. Li, Q. Han, The influence of alloy elements in Ti 6Al 4V and Ti 35Nb 2Ta 3Zr on the structure, morphology and properties of MAO coatings, Vacuum. 157 (2018) 229–236. https://doi.org/10.1016/j.vacuum.2018.08.054.
[137] G. Li, Y. Wang, S. Zhang, R. Zhao, R. Zhang, X. Li, C. Chen, Investigation on entrance mechanism of calcium and magnesium into micro-arc oxidation coatings developed on Ti-6Al-4V alloys, Surf Coat Technol. 378 (2019) 124951. https://doi.org/10.1016/j.surfcoat.2019.124951.
[138] D. Wei, Y. Zhou, D. Jia, Y. Wang, Effect of applied voltage on the structure of microarc oxidized TiO_2-based bioceramic films, Mater Chem Phys. 104 (2007) 177–182. https://doi.org/10.1016/j.matchemphys.2007.03.007.
[139] S. Lederer, P. Lutz, W. Fürbeth, Surface modification of Ti 13Nb 13Zr by plasma electrolytic oxidation, Surf Coat Technol. 335 (2018) 62–71. https://doi.org/10.1016/j.surfcoat.2017.12.022.
[140] Y. Wang, L. Wang, H. Zheng, C. Du, ChengyunNing, Z. Shi, C. Xu, Effect of frequency on the structure and cell response of Ca- and P-containing MAO films, Appl Surf Sci. 256 (2010) 2018–2024. https://doi.org/10.1016/j.apsusc.2009.09.041.
[141] W. Simka, R.P. Socha, G. Dercz, J. Michalska, A. Maciej, A. Krzakała, Anodic oxidation of Ti-13Nb-13Zr alloy in silicate solutions, Appl Surf Sci. 279 (2013) 317–323. https://doi.org/10.1016/j.apsusc.2013.04.091.
[142] J. Sun, Y. Han, X. Huang, Hydroxyapatite coatings prepared by micro-arc oxidation in Ca- and P-containing electrolyte, Surf Coat Technol. 201 (2007) 5655–5658. https://doi.org/10.1016/j.surfcoat.2006.07.052.
[143] S. Moon, Y. Jeong, Generation mechanism of microdischarges during plasma electrolytic oxidation of Al in aqueous solutions, Corros Sci. 51 (2009) 1506–1512. https://doi.org/10.1016/j.corsci.2008.10.039.
[144] S. Fujibayashi, M. Neo, H.-M. Kim, T. Kokubo, T. Nakamura, Osteoinduction of porous bioactive titanium metal, Biomaterials. 25 (2004) 443–450. https://doi.org/10.1016/S0142-9612(03)00551-9.
[145] J.H. Wang, J. Wang, Y. Lu, M.H. Du, F.Z. Han, Effects of single pulse energy on the properties of ceramic coating prepared by micro-arc oxidation on Ti alloy, Appl Surf Sci. 324 (2015) 405–413. https://doi.org/10.1016/j.apsusc.2014.10.145.
[146] M. Fazel, M. Shamanian, H.R. Salimijazi, Enhanced corrosion and tribocorrosion behavior of Ti6Al4V alloy by auto–sealed micro-arc oxidation layers, Biotribology. 23 (2020) 100131. https://doi.org/10.1016/j.biotri.2020.100131.

[147] S.A. Adeleke, S. Ramesh, A.R. Bushroa, Y.C. Ching, I. Sopyan, M.A. Maleque, S. Krishnasamy, H. Chandran, H. Misran, U. Sutharsini, The properties of hydroxyapatite ceramic coatings produced by plasma electrolytic oxidation, Ceram Int. 44 (2018) 1802–1811. https://doi.org/10.1016/j.ceramint.2017.10.114.
[148] W. Simka, A. Krząkała, D.M. Korotin, I.S. Zhidkov, E.Z. Kurmaev, S.O. Cholakh, K. Kuna, G. Dercz, J. Michalska, K. Suchanek, T. Gorewoda, Modification of a Ti-Mo alloy surface via plasma electrolytic oxidation in a solution containing calcium and phosphorus, Electrochim Acta. 96 (2013) 180–190. https://doi.org/10.1016/j.electacta.2013.02.102.
[149] E. Parfenov, L. Parfenova, V. Mukaeva, R. Farrakhov, A. Stotskiy, A. Raab, K. Danilko, N. Rameshbabu, R. Valiev, Biofunctionalization of PEO coatings on titanium implants with inorganic and organic substances, Surf Coat Technol. 404 (2020) 126486. https://doi.org/10.1016/j.surfcoat.2020.126486.
[150] R.C. Costa, J.G.S. Souza, J.M. Cordeiro, M. Bertolini, E.D. de Avila, R. Landers, E.C. Rangel, C.A. Fortulan, B. Retamal-Valdes, N.C. da Cruz, M. Feres, V.A.R. Barão, Synthesis of bioactive glass-based coating by plasma electrolytic oxidation: Untangling a new deposition pathway toward titanium implant surfaces, J Colloid Interface Sci. 579 (2020) 680–698. https://doi.org/10.1016/j.jcis.2020.06.102.
[151] G. Xu, X. Shen, Fabrication of SiO_2 nanoparticles incorporated coating onto titanium substrates by the micro arc oxidation to improve the wear resistance, Surf Coat Technol. 364 (2019) 180–186. https://doi.org/10.1016/j.surfcoat.2019.01.069.
[152] B. Zhang, B. Li, S. Gao, Y. Li, R. Cao, J. Cheng, R. Li, E. Wang, Y. Guo, K. Zhang, J. Liang, B. Liu, Y-doped TiO_2 coating with superior bioactivity and antibacterial property prepared via plasma electrolytic oxidation, Mater Des. 192 (2020) 108758. https://doi.org/10.1016/j.matdes.2020.108758.
[153] A. Zakaria, H. Shukor, M. Todoh, K. Jusoff, Bio-Functional Coating on Ti6Al4V Surface Produced by Using Plasma Electrolytic Oxidation, Metals (Basel). 10 (2020) 1124. https://doi.org/10.3390/met10091124.
[154] J. Yao, Y. Wang, G. Wu, M. Sun, M. Wang, Q. Zhang, Growth characteristics and properties of micro-arc oxidation coating on SLM-produced TC4 alloy for biomedical applications, Appl Surf Sci. 479 (2019) 727–737. https://doi.org/10.1016/j.apsusc.2019.02.142.
[155] A. Kazek-Kesik, M. Krok-Borkowicz, A. Jakóbik-Kolon, E. Pamuła, W. Simka, Biofunctionalization of Ti-13Nb-13Zr alloy surface by plasma electrolytic oxidation. Part II, Surf Coat Technol. 276 (2015) 23–30. https://doi.org/10.1016/j.surfcoat.2015.06.035.
[156] L. Chen, X. Jin, Y. Qu, K. Wei, Y. Zhang, B. Liao, W. Xue, High temperature tribological behavior of microarc oxidation film on Ti-39Nb-6Zr alloy, Surf Coat Technol. 347 (2018) 29–37. https://doi.org/10.1016/j.surfcoat.2018.04.062.
[157] A. v. Puz', S. v. Gnedenkov, N.G. Plekhova, R.E. Kostiv, T.S. Zaporozhets, V.S. Egorkin, S.L. Sinebryukhov, Chemical composition and osteogenerating properties of the bioactive coating on titanium alloy, AIP Conf Proc. 1874 (2017) 040043. https://doi.org/10.1063/1.4998116.
[158] Y. Wang, S. Zhao, G. Li, S. Zhang, R. Zhao, A. Dong, R. Zhang, Preparation and *in vitro* antibacterial properties of anodic coatings co-doped with Cu, Zn, and P on a Ti-6Al-4V alloy, Mater Chem Phys. 241 (2020) 122360. https://doi.org/10.1016/j.matchemphys.2019.122360.
[159] M. Thukkaram, P. Cools, A. Nikiforov, P. Rigole, T. Coenye, P. van der Voort, G. du Laing, C. Vercruysse, H. Declercq, R. Morent, L. de Wilde, P. de Baets, K. Verbeken, N. de Geyter, Antibacterial activity of a porous silver doped TiO_2 coating on titanium substrates synthesized by plasma electrolytic oxidation, Appl Surf Sci. 500 (2020) 144235. https://doi.org/10.1016/j.apsusc.2019.144235.
[160] B. Engelkamp, B. Fischer, K. Schierbaum, Plasma Electrolytic Oxidation of Titanium in H_2SO_4–H_3PO_4 Mixtures, Coatings. 10 (2020) 116. https://doi.org/10.3390/coatings10020116.
[161] S.-P. Kim, M. Kaseem, H.-C. Choe, Plasma electrolytic oxidation of Ti-25Nb-xTa alloys in solution containing Ca and P ions, Surf Coat Technol. 395 (2020) 125916. https://doi.org/10.1016/j.surfcoat.2020.125916.
[162] L. Meirelles, A. Arvidsson, M. Andersson, P. Kjellin, T. Albrektsson, A. Wennerberg, Nano hydroxyapatite structures influence early bone formation, J Biomed Mater Res A. 87A (2008) 299–307. https://doi.org/10.1002/jbm.a.31744.
[163] M. Kaseem, H.-C. Choe, The effect of in-situ reactive incorporation of MoOx on the corrosion behavior of Ti-6Al-4V alloy coated via micro-arc oxidation coating, Corros Sci. 192 (2021) 109764. https://doi.org/10.1016/j.corsci.2021.109764.
[164] T. Zehra, M. Kaseem, S. Hossain, Y.-G. Ko, Fabrication of a Protective Hybrid Coating Composed of TiO_2, MoO_2, and SiO_2 by Plasma Electrolytic Oxidation of Titanium, Metals (Basel). 11 (2021) 1182. https://doi.org/10.3390/met11081182.
[165] X. Li, M. Wang, W. Zhang, Y. Bai, Y. Liu, J. Meng, L. Zhang, A Magnesium-Incorporated Nanoporous Titanium Coating for Rapid Osseointegration, Int J Nanomedicine. 15 (2020) 6593–6603. https://doi.org/10.2147/IJN.S255486.
[166] M. Kaseem, H.-C. Choe, Triggering the hydroxyapatite deposition on the surface of PEO-coated Ti-6Al-4V alloy via the dual incorporation of Zn and Mg ions, J Alloys Compd. 819 (2020) 153038. https://doi.org/10.1016/j.jallcom.2019.153038.
[167] I.-J. Hwang, H.-C. Choe, Effects of Zn and Si ions on the corrosion behaviors of PEO-treated Ti-6Al-4V alloy, Appl Surf Sci. 477 (2019) 79–90. https://doi.org/10.1016/j.apsusc.2017.12.015.
[168] M. Kaseem, H.-C. Choe, Acceleration of Bone Formation and Adhesion Ability on Dental Implant Surface via Plasma Electrolytic Oxidation in a Solution Containing Bone Ions, Metals (Basel). 11 (2021) 106. https://doi.org/10.3390/met11010106.
[169] O. Yigit, N. Ozdemir, B. Dikici, M. Kaseem, Surface Properties of Graphene Functionalized TiO_2/nHA Hybrid Coatings Made on Ti6Al7Nb Alloys via Plasma Electrolytic Oxidation (PEO), Molecules. 26 (2021) 3903. https://doi.org/10.3390/molecules26133903.
[170] T. Zehra, M. Kaseem, Recent advances in surface modification of plasma electrolytic oxidation coatings treated by non-biodegradable polymers, J Mol Liq. 365 (2022) 120091. https://doi.org/10.1016/j.molliq.2022.120091.
[171] J.S. Dhaliwal, S.R.N. David, N.R. Zulhilmi, S.K. Sodhi Dhaliwal, J. Knights, R.F. de Albuquerque Junior, Contamination of titanium dental implants: a narrative review, SN Appl Sci. 2 (2020) 1011. https://doi.org/10.1007/s42452-020-2810-4.

[172] M. Qadir, Y. Li, K. Munir, C. Wen, Calcium Phosphate-Based Composite Coating by Micro-Arc Oxidation (MAO) for Biomedical Application: A Review, Critical Reviews in Solid State and Materials Sciences. 43 (2018) 392–416. https://doi.org/10.1080/10408436.2017.1358148.
[173] H.-T. Chen, H.-I. Lin, C.-J. Chung, C.-H. Tang, J.-L. He, Osseointegrating and phase-oriented micro-arc-oxidized titanium dioxide bone implants, J Appl Biomater Funct Mater. 19 (2021) 228080002110068. https://doi.org/10.1177/22808000211006878.
[174] Y. Han, S.-H. Hong, K. Xu, Structure and *in vitro* bioactivity of titania-based films by micro-arc oxidation, Surf Coat Technol. 168 (2003) 249–258. https://doi.org/10.1016/S0257-8972(03)00016-1.
[175] R.A. Gittens, R. Olivares-Navarrete, Z. Schwartz, B.D. Boyan, Implant osseointegration and the role of microroughness and nanostructures: Lessons for spine implants, Acta Biomater. 10 (2014) 3363–3371. https://doi.org/10.1016/j.actbio.2014.03.037.
[176] Q. Li, W. Yang, C. Liu, D. Wang, J. Liang, Correlations between the growth mechanism and properties of micro-arc oxidation coatings on titanium alloy: Effects of electrolytes, Surf Coat Technol. 316 (2017) 162–170. https://doi.org/10.1016/j.surfcoat.2017.03.021.
[177] J. Karbowniczek, F. Muhaffel, G. Cempura, H. Cimenoglu, A. Czyrska-Filemonowicz, Influence of electrolyte composition on microstructure, adhesion and bioactivity of micro-arc oxidation coatings produced on biomedical Ti6Al7Nb alloy, Surf Coat Technol. 321 (2017) 97–107. https://doi.org/10.1016/j.surfcoat.2017.04.031.
[178] R. Manoj Kumar, K.K. Kuntal, S. Singh, P. Gupta, B. Bhushan, P. Gopinath, D. Lahiri, Electrophoretic deposition of hydroxyapatite coating on Mg–3Zn alloy for orthopaedic application, Surf Coat Technol. 287 (2016) 82–92. https://doi.org/10.1016/j.surfcoat.2015.12.086.
[179] X.Z. Lin, M.H. Zhu, J.F. Zheng, J. Luo, J.L. Mo, Fretting wear of micro-arc oxidation coating prepared on Ti6Al4V alloy, Transactions of Nonferrous Metals Society of China (English Edition). 20 (2010) 537–546. https://doi.org/10.1016/S1003-6326(09)60175-8.
[180] F. Muhaffel, M. Kaba, G. Cempura, B. Derin, A. Kruk, E. Atar, H. Cimenoglu, Influence of alumina and zirconia incorporations on the structure and wear resistance of titania-based MAO coatings, Surf Coat Technol. 377 (2019) 124900. https://doi.org/10.1016/j.surfcoat.2019.124900.
[181] A.L. Yerokhin, X. Nie, A. Leyland, A. Matthews, Characterisation of oxide films produced by plasma electrolytic oxidation of a Ti6Al4V alloy, Surf Coat Technol. 130(2-3) (2000) 195-206. https://doi.org/10.1016/S0257-8972(00)00719-2.
[182] X. Zhang, Y. Wu, Y. Lv, Y. Yu, Z. Dong, Formation mechanism, corrosion behaviour and biological property of hydroxyapatite/TiO_2 coatings fabricated by plasma electrolytic oxidation, Surf Coat Technol. 386 (2020) 125483. https://doi.org/10.1016/j.surfcoat.2020.125483.
[183] R. Drevet, N. ben Jaber, J. Fauré, A. Tara, A. ben Cheikh Larbi, H. Benhayoune, Electrophoretic deposition (EPD) of nano-hydroxyapatite coatings with improved mechanical properties on prosthetic Ti6Al4V substrates, Surf Coat Technol. 301 (2016) 94–99. https://doi.org/10.1016/j.surfcoat.2015.12.058.
[184] S. Wang, Z. Ma, Z. Liao, J. Song, K. Yang, W. Liu, Study on improved tribological properties by alloying copper to CP-Ti and Ti-6Al-4V alloy, Mater Sci Eng C. 57 (2015) 123–132. https://doi.org/10.1016/j.msec.2015.07.046.
[185] K.G. Budinski, Tribological properties of titanium alloys, Wear. 151 (1991) 203–217. https://doi.org/10.1016/0043-1648(91)90249-T.
[186] K. Oguri, Fatigue life enhancement of aluminum alloy for aircraft by Fine Particle Shot Peening (FPSP), J Mater Process Technol. 211 (2011) 1395–1399. https://doi.org/10.1016/j.jmatprotec.2011.03.011.
[187] A. Kazek-Kęsik, G. Dercz, K. Suchanek, I. Kalemba-Rec, J. Piotrowski, W. Simka, Biofunctionalization of Ti-13Nb-13Zr alloy surface by plasma electrolytic oxidation. Part I, Surf Coat Technol. 276 (2015) 59–69. https://doi.org/10.1016/j.surfcoat.2015.06.034.
[188] M. Kaseem, H.-C. Choe, Electrochemical and bioactive characteristics of the porous surface formed on Ti-xNb alloys via plasma electrolytic oxidation, Surf Coat Technol. 378 (2019) 125027. https://doi.org/10.1016/j.surfcoat.2019.125027.
[189] M. Echeverry-Rendón, O. Galvis, R. Aguirre, S. Robledo, J.G. Castaño, F. Echeverría, Modification of titanium alloys surface properties by plasma electrolytic oxidation (PEO) and influence on biological response, J Mater Sci Mater Med. 28 (2017) 169. https://doi.org/10.1007/s10856-017-5972-x.
[190] S.J. Smith, R. Stevens, S. Liu, G. Li, A. Navrotsky, J. Boerio-Goates, B.F. Woodfield, Heat capacities and thermodynamic functions of TiO_2 anatase and rutile: Analysis of phase stability, Am Min. 94 (2009) 236–243. https://doi.org/10.2138/am.2009.3050.
[191] J. Takebe, S. Ito, S. Miura, K. Miyata, K. Ishibashi, Physicochemical state of the nanotopographic surface of commercially pure titanium following anodization-hydrothermal treatment reveals significantly improved hydrophilicity and surface energy profiles, Mater. Sci. Eng. C. 32 (2012) 55–60. https://doi.org/10.1016/j.msec.2011.09.011.
[192] C. Rey, C. Combes, C. Drouet, D. Grossin, Bioactive Ceramics: Physical Chemistry, in: Comprehensive Biomaterials, Elsevier, 2011: pp. 187–221. https://doi.org/10.1016/B978-0-08-055294-1.00178-1.
[193] T. Kokubo, H. Takadama, How useful is SBF in predicting *in vivo* bone bioactivity?, Biomaterials. 27 (2006) 2907–2915. https://doi.org/10.1016/j.biomaterials.2006.01.017.
[194] X. Chen, A. Nouri, Y. Li, J. Lin, P.D. Hodgson, C. Wen, Effect of surface roughness of Ti, Zr, and TiZr on apatite precipitation from simulated body fluid, Biotechnol Bioeng. 101 (2008) 378–387. https://doi.org/10.1002/bit.21900.
[195] J. Michalska, M. Sowa, M. Piotrowska, M. Widziołek, G. Tylko, G. Dercz, R.P. Socha, A.M. Osyczka, W. Simka, Incorporation of Ca ions into anodic oxide coatings on the Ti-13Nb-13Zr alloy by plasma electrolytic oxidation, Mater. Sci. Eng. C. 104 (2019) 109957. https://doi.org/10.1016/j.msec.2019.109957.
[196] M. Molaei, A. Fattah-alhosseini, M. Nouri, A. Nourian, Systematic optimization of corrosion, bioactivity, and biocompatibility behaviors of calcium-phosphate plasma electrolytic oxidation (PEO) coatings on titanium substrates, Ceram Int. 48 (2022) 6322–6337. https://doi.org/10.1016/j.ceramint.2021.11.175.

[197] H. Cimenoglu, M. Gunyuz, G.T. Kose, M. Baydogan, F. Uğurlu, C. Sener, Micro-arc oxidation of Ti6Al4V and Ti6Al7Nb alloys for biomedical applications, Mater Charact. 62 (2011) 304–311. https://doi.org/10.1016/j.matchar.2011.01.002.
[198] A. Pizzoferrato, G. Ciapetti, S. Stea, E. Cenni, C.R. Arciola, D. Granchi, Lucia, Cell culture methods for testing Biocompatibility, Clin Mater. 15 (1994) 173–190. https://doi.org/10.1016/0267-6605(94)90081-7.
[199] O. Oleshko, I. Liubchak, Y. Husak, V. Korniienko, A. Yusupova, T. Oleshko, R. Banasiuk, M. Szkodo, I. Matros-Taranets, A. Kazek-Kęsik, W. Simka, M. Pogorielov, *In Vitro* Biological Characterization of Silver-Doped Anodic Oxide Coating on Titanium, Materials. 13 (2020) 4359. https://doi.org/10.3390/ma13194359.
[200] C.E. Tanase, M. Golozar, S.M. Best, R.A. Brooks, Cell response to plasma electrolytic oxidation surface-modified low-modulus β-type titanium alloys, Colloids Surf B Biointerfaces. 176 (2019) 176–184. https://doi.org/10.1016/j.colsurfb.2018.12.064.
[201] X. Zhang, Z. Peng, X. Lu, Y. Lv, G. Cai, L. Yang, Z. Dong, Microstructural evolution and biological performance of Cu-incorporated TiO2 coating fabricated through one-step micro-arc oxidation, Appl Surf Sci. 508 (2020) 144766. https://doi.org/10.1016/j.apsusc.2019.144766.
[202] A. Santos-Coquillat, R. Gonzalez Tenorio, M. Mohedano, E. Martinez-Campos, R. Arrabal, E. Matykina, Tailoring of antibacterial and osteogenic properties of Ti6Al4V by plasma electrolytic oxidation, Appl Surf Sci. 454 (2018) 157–172. https://doi.org/10.1016/j.apsusc.2018.04.267.
[203] S. Guan, M. Qi, C. Wang, S. Wang, W. Wang, Enhanced cytocompatibility of Ti6Al4V alloy through selective removal of Al and V from the hierarchical micro-arc oxidation coating, Appl Surf Sci. 541 (2021) 148547. https://doi.org/10.1016/j.apsusc.2020.148547.
[204] K. Leśniak-Ziółkowska, A. Kazek-Kęsik, K. Rokosz, S. Raaen, A. Stolarczyk, M. Krok-Borkowicz, E. Pamuła, W. Simka, Plasma electrolytic oxidation as an effective tool for production of copper incorporated bacteriostatic coatings on Ti-15Mo alloy, Appl Surf Sci. 563 (2021) 150284. https://doi.org/10.1016/j.apsusc.2021.150284.
[205] K.E. Fox, N.L. Tran, T.A. Nguyen, T.T. Nguyen, P.A. Tran, Surface modification of medical devices at nanoscale—recent development and translational perspectives, in: Biomaterials in Translational Medicine, Elsevier, 2019: pp. 163–189. https://doi.org/10.1016/B978-0-12-813477-1.00008-6.
[206] D. Ding, Processing, properties and applications of ceramic matrix composites, SiC f /SiC, in: Advances in Ceramic Matrix Composites, Elsevier, 2014: pp. 9–25. https://doi.org/10.1016/B978-0-08-102166-8.00002-5.
[207] Z. Ranjbar, M. Bakhtiary-Noodeh, Electrophoretic deposition of waterborne colloidal dispersions, in: Handbook of Waterborne Coatings, Elsevier, 2020: pp. 181–194. https://doi.org/10.1016/B978-0-12-814201-1.00008-1.
[208] D.-S. Tsai, C.-C. Chou, Review of the Soft Sparking Issues in Plasma Electrolytic Oxidation, Metals (Basel). 8 (2018) 105. https://doi.org/10.3390/met8020105.